

# Explicit and Implicit Representations in AI-based 3D Reconstruction for Radiology: A systematic literature review

Yuezhe Yang<sup>a</sup>, Boyu Yang<sup>a</sup>, Yaqian Wang<sup>a</sup>, Yang He<sup>a</sup>, Xingbo Dong<sup>a,\*</sup>, Zhe Jin<sup>a</sup>

*<sup>a</sup>the Anhui Provincial International Joint Research Center for Advanced Technology in Medical Imaging, Anhui University, Hefei, 230093, Hefei, China*

---

## Abstract

The demand for high-quality medical imaging in clinical practice and assisted diagnosis has made 3D reconstruction in radiological imaging a key research focus. Artificial intelligence (AI) has emerged as a promising approach to enhancing reconstruction accuracy while reducing acquisition and processing time, thereby minimizing patient radiation exposure and discomfort and ultimately benefiting clinical diagnosis. This review explores state-of-the-art AI-based 3D reconstruction algorithms in radiological imaging, categorizing them into explicit and implicit approaches based on their underlying principles. Explicit methods include point-based, volume-based, and Gaussian representations, while implicit methods encompass implicit prior embedding and neural radiance fields. Additionally, we examine commonly used evaluation metrics and benchmark datasets. Finally, we discuss the current state of development, key challenges, and future research directions in this evolving field. Our project available on: <https://github.com/Bean-Young/AI4Med>.

*Keywords:* Radiological imaging, 3D reconstruction, Artificial intelligence, Explicit Representations, Implicit Representations

---

---

\*Corresponding author

## 1. Introduction

### 1.1. Development of Reconstruction Algorithms

Radiology involves a series of different tests to capture images of various parts of the body. A wide range of imaging examinations allows doctors to visualize the body's interior, including X-rays, MRI, ultrasound, CT scans, and PET scans [1]. Nowadays, radiological imaging modalities such as CT, MRI, and PET have been widely utilized for early disease detection, diagnosis, and treatment [2]. To convert signals collected by various sensors into images for analyzing biological processes in cells and tissues, image reconstruction algorithms are essential [3]. Among these, three-dimensional reconstruction algorithms are particularly important. They provide detailed 3D images of organs, which help detect infections, cancer, trauma, and abnormalities in blood vessels and organs [4].

Whats more, 3D reconstruction in radiological imaging research lies at the intersection of modern applied mathematics, engineering, medicine, radiology and computer science [5]. Initially, analysis methods based on continuous representations of the reconstruction problem were applied [6]. They using simple mathematical models to transform images into 3D. For example, the Filtered Back Projection (FBP) for CT [7] and the Fast Fourier Transform (FFT) [8] for MRI [9]. These algorithms are still considered foundational models today, as they offer computational efficiency and produce high-quality images under assumptions of noise-free and fully sampled data [10]. However, these physical-driven approaches typically focus only on the geometric structure and sampling characteristics of the imaging system [11]. They have high computational efficiency but are sensitive to noise, resulting in poor reconstruction quality.

To address this, more flexible reconstruction frameworks using Iterative Reconstruction (IR) methods were developed [12]. These methods provide better robustness to noise and incomplete data, though they come at the cost of increased computation [13]. As a result, many highly optimized algorithms incorporating data features have been introduced. One widely used example is the Ordered Subset Expectation Maximization (OSEM) algorithm [14] in PET imaging [15, 16], which is an accelerated variant of the Maximum Likelihood Expectation Maximization (MLEM) [17] algorithm that improves convergence speed and image quality. It improves convergence speed and computational efficiency by dividing the projection data into subsets and updating the model step by step. However, such traditional algorithms are

often limited in modeling complex anatomical structures and noise patterns, and their performance largely depends on high-quality scan data, which can be subject to randomness in clinical settings [18].

### *1.2. Advent of Neural Networks*

Fortunately, in recent years, artificial intelligence (AI) has gained significant attention due to its remarkable representational capacity and three-dimensional modeling capabilities [19]. This has led to a surge in research interest. Consequently, AI applications in 3D reconstruction for radiological imaging are now receiving unprecedented public attention [20, 21].

At its inception, convolutional neural networks (CNNs) [22] demonstrated a remarkable capacity for complex representation learning [23]. Concurrently, numerous methods began employing CNNs for 3D radiological image reconstruction [24]. Gong et al. integrated a deep residual CNN into an iterative reconstruction framework, enhancing PET image quality by leveraging inter-patient information [25]. However, CNNs exhibit limitations in sensitivity to positional information and struggle to capture global context [26], impeding their application in medical image reconstruction tasks. Inspired by the Transformer [27] architecture, the introduction of Vision Transformers (ViT) [28] effectively addresses these challenges, establishing itself as a new benchmark in the field of medical image analysis [29].

However, ViT is primarily designed for feature extraction and faces difficulties when directly applied to reconstruction tasks [30]. Moreover, the self-attention mechanism of ViT imposes high computational demands, especially when processing high-resolution and complex medical images, potentially leading to efficiency concerns [30].

### *1.3. Rise of Generative Models*

In sharp contrast, advancements in generative modeling have offered alternative solutions in a different domain. One such approach is the Variational Autoencoder (VAE) [31], which learns a probabilistic latent space to generate new data samples by approximating the data distribution. In parallel, Generative Adversarial Networks (GAN) [32], first introduced in 2014, utilize adversarial training between two neural networks to generate realistic data samples. Their exceptional performance in generation tasks has attracted significant attention in 3D reconstruction for radiological imaging [6]. By

combining GAN with CNNs and ViT, Luo et al. proposed the Transformer-GAN framework to reconstruct high-quality standard-dose PET images from low-dose PET images with superior performance [33].

Despite the robustness of the GAN architecture in enhancing image clarity and detail, its inherent instability during training can cause unnatural artifacts [34]. These inconsistencies can be detrimental to medical imaging applications. Diffusion models, in contrast, use a noise-based framework, gradually adding noise to data until it becomes random [35]. By learning a reverse process to iteratively denoise and recover the original data, new samples are generated in the process. This framework generally exhibits greater training stability, making diffusion models a promising new solution for 3D reconstruction in radiological imaging [36]. For instance, AdaDiff introduces an adaptive diffusion prior for accelerated MRI reconstruction, addressing challenges posed by domain shifts in imaging operators and MRI image distributions [37].

However, diffusion models struggle to account for consistency across different viewpoints [38]. Their high computational complexity and challenges in directly generating 3D models often result in suboptimal outcomes for 3D medical imaging. Explicit generation methods, such as these, often fail to address the lack of internal detail and resolve issues related to viewpoint consistency [39].

#### *1.4. Emergence of Novel Representations*

In 2020, Neural Radiance Fields (NeRF) gained significant attention in the natural image domain for novel view synthesis tasks, making implicit generative models a viable solution [40]. For example, MedNeRF combines NeRF with GAN to reconstruct 3D-aware CT projections from single or few-view X-rays [41]. This network can significantly reduce patient exposure to ionizing radiation while maintaining high-fidelity anatomical representations for medical applications.

While NeRF excels in reconstructing 3D scenes with strong spatial consistency, its slow rendering speed makes it unsuitable for real-time imaging in radiological medicine [42]. In 2023, the 3D Gaussian Splatting (3DGS) framework introduced a explicit radiance field methods for novel view synthesis in natural images [43]. This framework achieves high accuracy while enabling real-time image rendering [44], paving the way for its application in medical imaging. For instance,  $R^2$ -Gaussian is an innovative 3D Gaussian splatting framework optimized for sparse-view tomographic reconstruction,

effectively addressing integration biases [45]. It achieves superior accuracy and efficiency in volumetric imaging while minimizing computational time.

In summary, over the past decades, advancements in artificial intelligence have significantly impacted the field of 3D reconstruction in radiological imaging, leading to a variety of innovative approaches. The developmental roadmap is shown in Fig.1. Thus, it is essential to summarize existing research and conduct a comprehensive comparison and analysis of methods in this field, providing a reference for future studies.

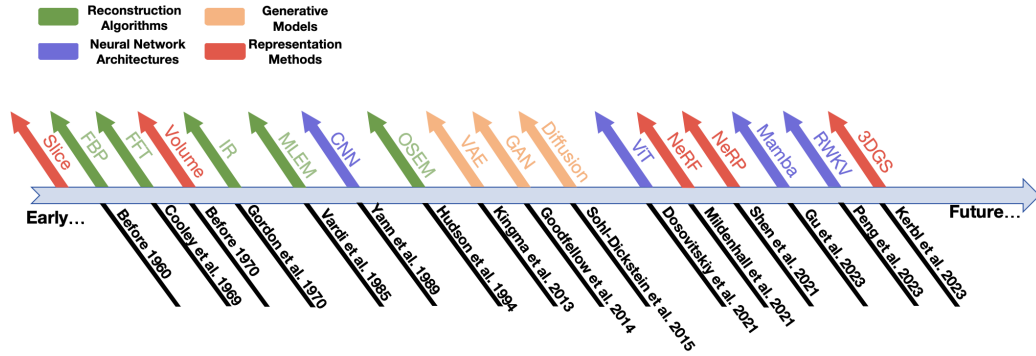


Figure 1: A brief chronology of the development of techniques related to radiological image reconstruction in literature.

However, existing reviews often focus on specific models or summarize only a subset of technologies, frequently overlooking implicit imaging methods [46, 6, 47]. This narrow focus makes it difficult for readers to comprehensively understand the integration of radiological imaging with computer science and its technological developments. This review aims to provide a comprehensive overview of the application of artificial intelligence in 3D reconstruction for radiological imaging, encompassing two main categories: explicit reconstruction and implicit reconstruction. The differences between these two methods are shown in Fig.2. By collecting relevant literature from the past five years, this study explores the key challenges and solutions in the field, offering a reliable reference for researchers. The survey covers a wide range of radiological imaging modalities, including 3D ultrasound, CT, MRI, PET, and SPECT. Based on the current key issues in these studies, we present a comprehensive summary of existing methodologies. The primary contributions of this review are as follows:

- Includes radiological imaging of various anatomical regions and almost all AI-based 3D reconstruction methods in this domain.
- From the perspective of integrating computer graphics with medical science, the review classifies existing methods based on the morphology reconstructed into two categories: explicit reconstruction and implicit reconstruction. This is also the first review to incorporate implicit reconstruction methods comprehensively.
- The review identifies and summarizes 65 publicly available datasets, representing the largest-scale dataset summary in current reviews.
- It proposes future research directions for the field.

The remainder of this survey is organized into seven sections. Section 2 describes the literature research methodology. Section 3 introduces publicly available datasets and evaluation metrics. Section 4 summarizes the applications of explicit reconstruction methods in 3D radiological imaging. Section 5 focuses on the applications of implicit reconstruction methods. Section 6 discusses current challenges, future research directions, and Section 7 concludes the review.

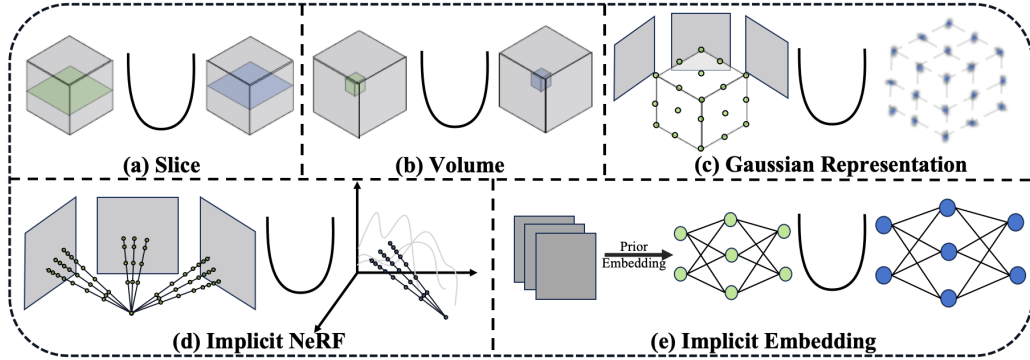


Figure 2: Five different forms of reconstruction representations in radiological imaging, with the first row showing explicit representations and the second row implicit ones.

## 2. Methods

### 2.1. Literature Review

The research on 3D reconstruction in radiological imaging and artificial intelligence primarily draws from the following databases: Web of Science

[48], Google Scholar [49], and Scopus [50]. The search encompasses publications from the past five years.

Initially, the search results are refined using filtering criteria, such as article type and research field, to narrow the number of results. Next, duplicate records are excluded. Subsequently, the records are screened based on their titles, abstracts, and the study selection criteria. Studies that cannot be retrieved are then excluded. Finally, 65 studies that meet the inclusion criteria are incorporated into the systematic review. Fig.3 illustrates the flowchart of the systematic literature review. The distribution of these studies by year is depicted in Fig.5(a).

In Fig.3, our search keywords include artificial intelligence, deep learning, 3D, medical imaging, and imaging reconstruction. Only research articles that contain all these keywords are included in our study. we apply three selection criteria: **1)** Research content filtering: Papers are selected based on their intrinsic research focus. We rigorously evaluate the relevance of each paper to ensure it is representative and relevant to our research scope. **2)** Citation count: We assess the citation count of each paper. Higher citation counts are prioritized, as a higher citation count often reflects greater recognition and impact within the field. **3)** Representative journals or conferences: Priority is given to papers published in prestigious journals or leading conferences, such as *IEEE Transactions on Medical Imaging (T-MI)*, *Medical Image Analysis (MedIA)*, *The IEEE/CVF Conference on Computer Vision and Pattern Recognition (CVPR)*, *International Conference on Medical Image Computing and Computer Assisted Intervention (MICCAI)* and etc. This criterion guarantees that the selected literature has been subjected to rigorous peer review, ensuring its credibility.

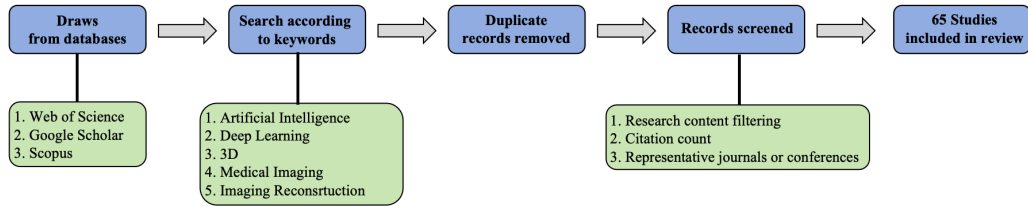


Figure 3: Flowchart of the literature review.

## 2.2. Literature Classification

There are multiple feasible classification criteria for studies on radiological image 3D reconstruction [46, 51]. One approach is based on imaging modalities, where studies are categorized according to their focus on CT, MRI, PET, SPECT, US, or multimodal imaging, as illustrated in Fig.5(b). Another classification considers the targeted anatomical regions, distinguishing studies that focus on brain imaging, breast imaging, or whole-body imaging. A third approach categorizes studies based on reconstruction tasks, which can generally be divided into three types, as shown in the Fig.4. **Task I** involves reconstructing 3D images from raw data, primarily aimed at accelerating the imaging process. **Task II** focuses on transforming low-dose images into normal-dose images, with the goal of enhancing resolution or reducing artifacts. **Task III** involves reconstructing images from missing signals, aiming to restore complete images using limited perspective information. While these classification schemes offer valuable insights, they do

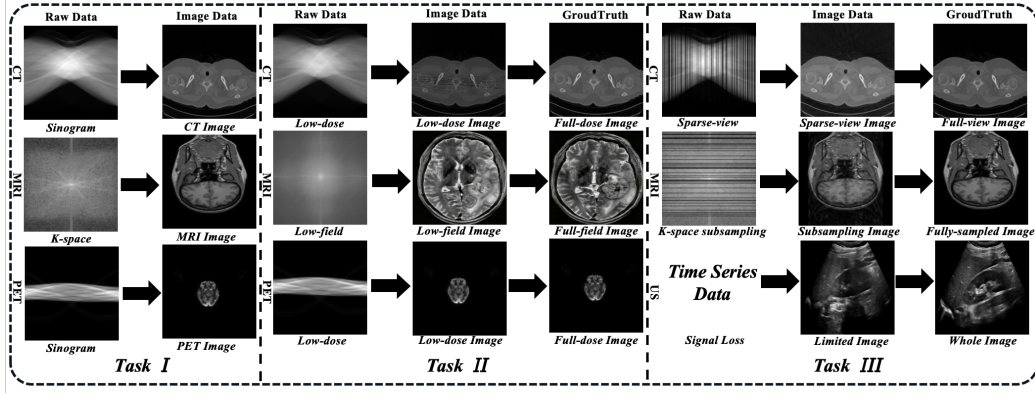


Figure 4: Three distinct types of tasks in radiological image reconstruction.

not address methodological considerations from an artificial intelligence perspective. In the context of 3D representation, reconstruction methods can be categorized as explicit or implicit. Explicit representations use directly observable formats, such as points, volumes, or Gaussian representations which are inherently discrete. In particular, Gaussian representations integrate maintaining a discrete structure between points while preserving continuity within individual points. Implicit representations, in contrast, rely on continuous functions, such as neural radiance fields, to model imaging in a



non-intuitive manner. From this AI-driven perspective, we re-examined medical image 3D reconstruction and classified methods based on their output representations into explicit and implicit reconstructions. The classification results based on this criterion are shown in Fig.5(c). **And in this work, we innovatively classify literature based on representations.**

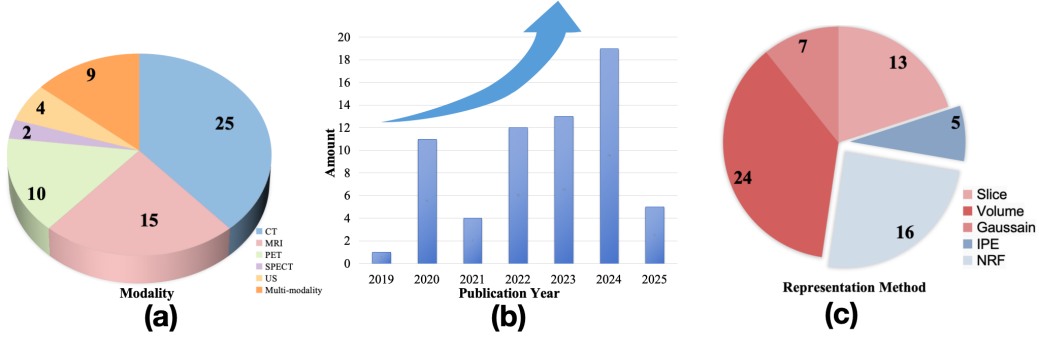


Figure 5: Categorization results of the reviewed literature, including: (a) classification based on imaging modalities, (b) publication year, and (c) representation forms used in reconstruction methods.

### 3. Datasets and metrics

#### 3.1. Datasets

In the task of 3D reconstruction in radiological imaging, publicly available datasets play a crucial role [52]. High-quality, standardized data is essential for algorithm training, validation, and testing. Public datasets provide researchers with a unified benchmark, enabling fair comparisons of different methods under the same conditions, thereby facilitating algorithm optimization and advancement [53].

Unlike other medical imaging tasks, reconstruction often requires subjects to undergo two scans under comparable conditions, particularly maintaining consistent positioning, posture, and physiological state, in order to obtain corresponding test samples and ground truth data. Additionally, medical data is subject to strict legal and regulatory constraints due to patient privacy concerns [54], making data collection both challenging and costly. The availability of public datasets significantly lowers the barrier to data access. Our review provides the most comprehensive publicly available datasets for 3D reconstruction in radiological imaging tasks, including

CT [55, 56, 57, 58, 59, 60, 61, 62, 63, 64, 41], MRI [65, 66, 67, 68, 69, 70, 71, 72, 73, 74, 75, 76, 77, 78, 79, 80, 81, 82, 83, 84, 85, 86], PET [87], US [88, 89, 90], and multi-modality [91, 92, 93] datasets. The specific details are presented in Table 1.

Table 1: Open access dataset for 3D reconstruction radiological imaging tasks

Modalities	Dataset	Size	Detail
CT	VerSe [55, 56, 57]	355	A multi-center, multi-detector CT spine dataset for vertebral annotation and segmentation.
	LIDC-IDRI [58]	1010	A low-dose lung CT dataset for lung nodule classification, segmentation, and detection.
	COVID-CT-Dataset [59]	216	Dataset that contains COVID-19 CT images and non-COVID-19 CTs.
	Richard et al. [60]	6762	volumetric reconstructions of the chest cavity at 10 breathing phases .
	KiTS19 [61]	300	Dataset of segmented CT imaging for automatic semantic segmentation of renal tumors and surrounding anatomy.
	LDCT [62]	299	CT projection data, including those acquired at routine clinical doses and simulated lower doses.
	CTSpine1K [63]	1005	Dataset curated from mutiple sources for spinal vertebrae segmentation and 3D spine reconstruction.
	MIDRC-RICORD-1B [64]	117	De-identified dataset from COVID negative patients.
	Corona-Figueroa et al. [41]	25	Digital Reconstructed Radiographs from chest and knee CT scans.
MRI	BraTS [65, 66, 67, 68, 69, 70]	2040	Brain MRI scans from patients with gliomas, including four modalities: T1-weighted , contrast-enhanced T1-weighted , T2-weighted , and T2-FLAIR .
	IXI [71]	600	T1, T2 and PD-weighted images, MRA and Diffusion-weighted images from normal, healthy subjects.
	ADNI [72]	8320	A collection of longitudinal clinical, imaging, genetic, and other biomarker data.
	OASIS-1 [73]	436	MRI Data from Young, Middle-Aged, Nondemented, and Demented Older Adults in a Cross-Sectional Study.
	FastMRI [74, 75]	8470	Dataset that include K-space and image data of knee for accelerated MR image reconstruction using machine learning.
	HCP [76]	1200	High-level extensively processed datasets featuring group average structural and tfMRI data, functional connectivity, and Group ICA-based parcellation, timeseries, and netmats datasets.
	Landman et al. [77]	21	Dataset featuring MPRAGE, FLAIR, DTI, resting state fMRI, B0 and B1 field maps, ASL, VASO, quantitative T1 mapping, quantitative T2 mapping, and magnetization transfer imaging.

*Continued on next page*

Modalities	Dataset	Size	Detail
	dHCP [80]	1056	Anatomical, diffusion, and functional metadata, including brain segmentation and cortical surface.
	MSD [81]	750	Multiparametric MRI scans from glioblastoma and lower-grade glioma.
	BreastDM [82]	232	DCE-MR images for benign and malignant breast tumor cases.
	OCMR [83]	377	Multi-coil k-space data and undersampled cardiac cine series.
	SKMTEA [84]	155	A dataset that integrates raw quantitative knee MRI data, corresponding image data, and detailed annotations of tissue and pathology, facilitating an end-to-end investigation and assessment of the MRI imaging process.
	CMRxRecon2024 [94]	330	Dataset that includes multi-contrast k-space data for multi-contrast CMR reconstruction and random sampling CMR reconstruction .
PET	UDPET [87]	1447	A dataset that includes 18F-FDG PET imaging for addressing the challenges of ultra-low dose imaging in whole-body PET imaging.
US	Wysocki et al. [88]	18	A dataset of synthetic liver ultrasound images and tracked spine phantom scans.
	MITEA [89]	134	The dataset is designed for the quantification of LV systolic function and mass using annotated 3D echocardiography data.
	Papageorgiou et al. [90]	13,108	A set of international standards for fetal growth to enhance the accuracy of diagnosing fetal growth restriction and improve clinical management .
CT MRI	MMWHS [91]	120	Three-dimensional CT and MRI images covering the entire heart for cardiac segmentation.
MRI PET	OASIS-3 [92]	1379	Neuroimaging and processed imaging data from individuals experiencing normal aging and those with Alzheimer’s Disease.
MRI US	-RegPro [93]	141	Dataset for assisting prostate biopsy and focal therapy, surgical and interventional tasks.

### 3.2. Metrics

Evaluation metrics play a critical role in the study of medical image reconstruction by providing standardized assessment, guiding algorithm optimization, and validating clinical applicability. Scientifically sound and well-designed metrics enable an objective evaluation of reconstruction fidelity, detail preservation, and noise suppression, ensuring the practical utility of models across different application scenarios[95]. Since different metrics focus on distinct aspects of image quality[96], a single metric is often insufficient to comprehensively reflect reconstruction performance. Therefore, a combination of multiple metrics is typically required for a more thorough and

reliable evaluation. This review summarizes the commonly used metrics in 3D reconstruction for radiological image tasks, with the results presented in Table 2.

Table 2: Evaluation metrics for radiological image reconstruction

Name	Formula	Function
Mean Squared Error (MSE) ↓	$MSE = \frac{1}{N} \sum_{i=1}^N (x_i - y_i)^2$	Measures pixel-wise intensity differences.
Root Mean Squared Error (RMSE) ↓	$RMSE = \sqrt{MSE}$	Square root of MSE.
Normalized Root Mean Square Error (NRMSE) ↓	$NRMSE = \frac{\sqrt{MSE}}{\max(x) - \min(x)}$	Normalized MSE for different intensity ranges.
Peak Signal-to-Noise Ratio (PSNR) ↑	$PSNR = 10 \log_{10} \frac{\max(x)^2}{MSE}$	Evaluates image quality based on signal strength.
Structural Similarity Index (SSIM) ↑	$SSIM(x, y) = \frac{(2\mu_x\mu_y + C_1)(2\sigma_{xy} + C_2)}{(\mu_x^2 + \mu_y^2 + C_1)(\sigma_x^2 + \sigma_y^2 + C_2)}$	Measures structural similarity between images. Ranges from -1 to 1;
Learned Perceptual Image Patch Similarity (LPIPS) ↓	$LPIPS(x, y) = \sum_l w_l \cdot \ F_l(x) - F_l(y)\ _2^2$	Measures perceptual similarity based on deep learning.
Mean Absolute Error (MAE) ↓	$MAE = \frac{1}{N} \sum_{i=1}^N  x_i - y_i $	Measures absolute intensity differences.
Feature Similarity Index (FSIM) ↑	$FSIM = \frac{\sum_{x,y} PC_m(x,y) \cdot S_L(x,y) \cdot S_C(x,y)}{\sum_{x,y} PC_m(x,y)}$	Evaluates perceptual quality with structural information.
Signal-to-Noise Ratio (SNR) ↑	$SNR = 10 \log_{10} \frac{\sum_{i=1}^N x_i^2}{\sum_{i=1}^N (x_i - y_i)^2}$	Measures signal clarity relative to noise.
Contrast-to-Noise Ratio (CNR) ↑	$CNR = \frac{ \mu_R - \mu_B }{\sigma_B}$	Evaluates contrast between regions of interest.
Cosine Similarity (CS) ↑	$CS = \frac{\sum x_i y_i}{\sqrt{\sum x_i^2} \cdot \sqrt{\sum y_i^2}}$	Measures the cosine of the angle between two image feature vectors.
Computation Time (Time) ↓	Measured in seconds	Evaluates computational efficiency.
Rendering Speed (Speed) ↑	Frames per second (FPS)	Measures the speed of rendering in frames per second.
Model Parameters (Para.) ↓	Count of model parameters	Evaluates the complexity and size of the model.

The definitions of the symbols used in Table 2 are as follows:  $x_i$  and  $y_i$  represent the pixel intensity values or feature vector components of the original and reconstructed images respectively, and  $N$  denotes the total number of pixels. The means and variances of images  $x$  and  $y$  are represented by  $\mu_x$ ,  $\mu_y$  and  $\sigma_x^2$ ,  $\sigma_y^2$  respectively, and  $\sigma_{xy}$  is their covariance. And  $\max(x)$  and  $\min(x)$  represent the maximum and minimum intensity values in the image. The constants  $C_1$  and  $C_2$  are small positive stabilizing constants used in the SSIM calculation. In LPIPS,  $F_l(x)$  and  $F_l(y)$  represent the feature maps at layer  $l$ , and  $w_l$  denotes the learned weight for each layer. FSIM is computed

based on phase congruency  $PC_m(x, y)$ , a contrast-based feature, along with luminance similarity  $S_L(x, y)$  and contrast similarity  $S_C(x, y)$ . For CNR,  $\mu_R$  and  $\mu_B$  represent the mean intensities of the regions of interest (ROI) and background.  $\sigma_B$  denotes the standard deviation of the background intensity.

Table 2 presents a comprehensive set of evaluation metrics for medical image reconstruction, categorized into pixel-wise error, signal and noise, perceptual similarity, and computational performance metrics. Pixel-wise error metrics, such as MSE, RMSE, NEMSE and MAE, quantify intensity differences between reconstructed and reference images. Signal and noise metrics, including PSNR, SNR and CNR, assess the clarity and contrast of images relative to noise levels. Perceptual and structural similarity metrics, like SSIM, LPIPS, FSIM and CS, capture the high-level structural and perceptual quality of images. Finally, computational performance metrics, such as Time, Speed and Para. evaluate the efficiency and feasibility of the reconstruction method in practical applications. Together, these indicators provide a balanced assessment of image quality, structural fidelity, and computational cost in medical image reconstruction.

#### 4. Explicit reconstruction methods

Explicit representations were initially used for AI-assisted reconstruction of radiological imaging. At first, the most typical explicit reconstruction methods were slice-based, meaning that experiments were conducted using individual slices. This representation was widely applied in CT [97?, 98], MRI [99, 100, 101, 102], PET [103, 104, 105] and SPECT [106] imaging, with potential for multi-modality [107, 108] applications. More details are shown in Table 3. However, such methods overlooked the longitudinal continuity of radiology images, leading to severe artifacts or inconsistencies across slices. Later, volume-based reconstruction methods emerged. Unlike slice-based approaches, volume representations incorporate spatial information at each location, enabling more accurate restoration of radiology images. This representation is applicable to all three-dimensional imaging modalities, including CT [109, 110, 111, 112, 113, 114, 115, 116], MRI [117, 118, 119, 120, 121, 122, 123, 124, 125], PET [126, 127, 128, 129, 130], SPECT [131] and multi-modality [132]. More details are shown in Table 4. Recently, an explicit Gaussian representation integrated with neural radiance field concepts, known as 3DGS [43], has gained significant attention in radiological imaging due to its precise representation and high reconstruction

efficiency [133]. It has been widely applied in CT [134, 135, 45, 136, 137, 138] image reconstruction and explored for multi-modality [139] applications. The specific detail can be found in Table 5. Next, we will discuss representative papers from different perspectives.

#### 4.1. Slice-base Representation

The slice-based method reconstructs images in a single direction, with early deep learning approaches relying on CNN-based U-Net [140] architectures. Du et al. [99] introduced a CNN model with residual learning and skip connections, effectively addressing gradient vanishing and achieving superior PSNR and SSIM compared to traditional methods. Their model also enabled multi-modality super-resolution by reconstructing T2-weighted MRI from T1-weighted MRI training. With the rise of ViTs in computer vision [28], Shi et al. proposed CTTR [97], a Transformer-based sparse-view CT reconstruction method that reduces artifacts and detail loss. CTTR outperformed CNN-based methods in PSNR and SSIM under extremely sparse-view conditions.

Mamba [141], a state-space model for efficient sequence processing, has recently gained attention. Building on this, MambaMIR [107] adapts Mamba for medical image reconstruction, leveraging its linear complexity, global receptive fields, and dynamic weighting. It introduces an Arbitrary-Masked Mechanism, enhancing its suitability for medical imaging, and incorporates Monte Carlo-based uncertainty estimation. Experiments show that MambaMIR achieves SOTA or superior performance in Fast MRI and Sparse-View CT tasks, effectively handling long-sequence data while optimizing computational efficiency for large-scale medical image reconstruction.

Although Mamba has unidirectionality issues, making it difficult to model both global and local dependencies in 2D images efficiently. In recent years, the Receptance Weighted Key Value (RWKV) model [142] introduced WKV attention, enabling long-range dependencies while maintaining linear computational complexity. Restore-RWKV incorporates a Token Shift layer to enhance local feature capture. Restore-RWKV [108] is the first RWKV-based medical image restoration model, designed to address high computational complexity and insufficient global information capture in high-resolution medical imaging.

The advantage of this slice-based reconstruction method is its versatility, as the model can adapt to different imaging modalities. With the advancement of deep learning models, this approach will increasingly focus on

efficiency and accuracy.

#### 4.2. Volume-base Representation

Volume-based representations describe 3D structures using numerous small volumetric elements [143, 144]. This approach enables high-fidelity, detail-rich radiology image reconstruction through direct processing of volumetric data. In medical applications, this approach precisely captures complex anatomical structures within the human body.

Although volume-based reconstruction has employed UNet networks for generation, this section focuses on more advanced generative models.

GANs train through an adversarial process between a generator and a discriminator [32], allowing the generator to produce high-quality data that matches the real data distribution.

In radiology image reconstruction, Shaul et al. [119] proposed a GAN-based undersampled MRI reconstruction method that accelerates MRI acquisition while maintaining anatomical image quality. They optimized reconstruction with fidelity loss, image-quality loss, and adversarial loss, generating more realistic and natural MRI images. Experiments demonstrated that this method can reconstruct high-quality brain MRI with fivefold acceleration.

Similarly, X2CT-GAN [109] leverages GANs to reconstruct 3D CT images from biplanar X-rays, reducing radiation exposure and the high costs of traditional CT scans. By incorporating a feature fusion module to integrate information from different views, the method enhances reconstruction quality. Experiments showed a 4dB improvement in PSNR and superior SSIM performance compared to CNN-based methods.

Despite GANs effectiveness, they suffer from mode collapse and unstable training [145]. Diffusion models [146, 147, 148, 149], optimized via Markov chains and variational inference, stabilize the generation process by progressively adding noise and learning the denoising process, achieving broader coverage of the real data distribution.

Chung et al. introduced DiffusionMBIR [132], which combines pretrained 2D diffusion models with model-based iterative reconstruction for sparse-view CT, limited-angle CT, and compressed sensing MRI. By integrating a 2D diffusion prior with 3D total variation regularization, the approach significantly improves 3D reconstruction quality. Experimental results show that DiffusionMBIR maintains high-quality reconstruction even with extreme

data sparsity, such as two-view CT reconstruction, outperforming existing diffusion and deep learning methods in PSNR and SSIM.

In the PET domain, Gong et al. [130] proposed a denoising diffusion probabilistic model (DDPM)-based method for PET image denoising. By progressively adding noise and iteratively denoising during the reverse process, this approach achieves high-quality PET image reconstruction. Results indicate that DDPM outperforms traditional methods such as non-local means (NLM), UNet, and GANs in both PSNR and SSIM.

Due to its ability to explicitly represent 3D information with high accuracy [150, 151], the volume representation approach is widely adopted. However, its computational complexity poses challenges for real-time imaging [152, 153]. Future research will continue striving for fast and accurate volume-based reconstruction.

#### 4.3. Gaussian Representation

Unlike other explicit representation reconstruction methods, Gaussian representations model 3D scenes with millions of learnable 3D Gaussian Points, enabling real-time medical image rendering with exceptional editability through differentiable rendering [154]. X-Gaussian pioneers the integration of 3DGS in medical imaging by eliminating view dependency and introducing an angle-pose cuboid initialization strategy. It achieves a 6.5 dB PSNR improvement, 73 faster inference, and 85% shorter training time than state-of-the-art methods [138]. DDGS-CT further enhances accuracy by decomposing radiosity into isotropic and directional components and employing a radiodensity-aware dual sampling strategy [137]. It surpasses X-Gaussian in PSNR and SSIM while using fewer Gaussians and rendering at 7.46 ms per frame. It also improves intraoperative 2D/3D registration, reducing landmark alignment errors by 62% compared to analytical DRR techniques. While primarily applied to CT imaging, extending this cutting-edge Gaussian representation to MRI, PET, and other modalities could revolutionize medical imaging reconstruction.

Table 3: Related works on slice-based radiological image reconstruction.

Modality	Paper	Year	Detail
	CTTR [97]	2022	A dual-domain deep learning model for sparse-view CT reconstruction, using Transformers to improve images quality with sinogram features.

CT

*Continued on next page*



Modality	Paper	Year	Detail
	DuDoTrans [155]	2022	Utilize the long-range dependency modeling capability of the Transformer to restore informative sinograms, and subsequently reconstruct the CT image using both the enhanced sinograms and the original sinograms.
	CoreDiff [98]	2023	A diffusion-based model using a mean-preserving degradation operator and CLEAR-Net for low-dose CT denoising, enhancing image quality with fewer sampling steps.
MRI	Du et al. [99]	2020	A deep learning model using residual learning and skip connections for super-resolution reconstruction of 3D MRI images.
	SLATER [100]	2022	Introduce an unsupervised MRI reconstruction method using adversarial transformers to learn MRI priors and perform zero-shot inference for improved image quality.
	PCNN [101]	2021	A perceptual complex neural network for rapid reconstruction of undersampled MRI data using complex convolution and perceptual loss.
	Wei et al. [102]	2022	An unsupervised deep learning model for real-time 3D MRI reconstruction from cine-MRI, using deformation vector fields to estimate respiratory motion.
PET	MCAD [103]	2024	A multi-modal conditioned adversarial diffusion model for reconstructing high-quality PET images from low-dose PET and clinical data using diffusion processes and semantic consistency.
	MEaTransGAN [104]	2024	An original deep learning model that integrates CNNs, Transformer, and GANs to reconstruct high-quality standard-dose PET images utilizing low-dose PET and T1-MRI images, enhancing diagnostic value while reducing radiation exposure.
	Singh et al. [105]	2024	A 3D PET reconstruction framework using score-based generative models with a novel PET-DDS sampling method to improve image quality and robustness.
SPECT	TPL-CNN [106]	2024	An iterative deep denoising method using a GAN-based approach improves SPECT myocardial perfusion imaging by reducing noise and enhancing contrast during reconstruction.
CT MRI	MambaMIR [107]	2025	Improving global sensitivity and uncertainty quantification in medical image reconstruction using Monte Carlo arbitrary-masked Mamba.
CT MRI PET	Restore-RWKV [108]	2024	Restore-RWKV cleverly incorporates a recurrent WKV attention mechanism with linear computational complexity and an omnidirectional token shift mechanism.

Table 4: Related works on volume-based radiological image reconstruction.

Modality	Paper	Year	Detail
CT	X2CT-GAN [109]	2019	A GAN-based model that reconstructs high-resolution 3D CT images from biplanar 2D X-rays using a specially designed generator and combined loss functions.
	DEER [110]	2020	Introduce a highly efficient deep learning model for few-view breast CT reconstruction, achieving high image quality with low model complexity.
	HDNet [111]	2020	A hybrid-domain neural network approach for SVCT reconstruction, suitable for cone-beam CT imaging with low memory demands.

*Continued on next page*

Modality	Paper	Year	Detail
	Singh et al. [112]	2020	DLR outperforms commercial IR and FBP in image quality and lesion detection when used at submillisievert doses for chest and abdominopelvic CT.
	DLR [113]	2020	While maintaining noise texture and spatial resolution, DLR significantly enhances image quality and reduces radiation dose in pediatric CT examinations.
	DIOR [114]	2022	DIOR integrates iterative optimization and deep residual learning to enhance limited-angle CT reconstruction, improving artifact removal and detail preservation.
	FreeSeed [115]	2023	Propose a frequency-band-aware and self-guided network to effectively remove artifacts and restore details in sparse-view CT images.
	C <sup>2</sup> RV [116]	2024	A multi-scale volumetric representation with scale-view cross-attention enables adaptive feature aggregation for improved 3D learning.
MRI	Pezzotti et al. [117]	2020	Adaptive intelligence enhances MRI reconstruction by integrating domain knowledge with deep learning, achieving top rankings in the fastMRI challenge.
	EMISR [118]	2020	Three hidden layers extracted from a super-resolution CNN are integrated with a sub-pixel convolution layer sourced from an efficient sub-pixel CNN.
	Shaul et al. [119]	2020	High-quality MRI reconstruction is realized through the proposed framework by synergistically combining U-Net and GAN architectures.
	T-Net [120]	2020	High-quality MRI images can be reconstructed from undersampled data through the mapping function implemented by the Volume Depth Residual Network.
	MADGAN [121]	2021	Propose a GAN-driven approach for reconstructing multiple adjacent brain MRI slices, enabling anomaly detection across different stages in multi-sequence structural MRI scans.
	AUTOMAP [122]	2021	An end-to-end deep neural network framework is employed in to enhance the image quality of low-field MRI data severely degraded by noise.
	CINENet [123]	2020	A novel 4D deep reconstruction framework achieves efficient generation of high-quality isotropic 3D CINE MRI from single breath-hold acquisitions, demonstrating enhanced contrast and accelerated reconstruction.
	Recon3DMLP [124]	2023	The architecture combines CNN modules employing small kernels for low-frequency reconstruction with adaptive MLP modules utilizing large kernels to enhance high-frequency reconstruction.
	Li et al. [125]	2024	This MRI super-resolution method uniquely integrates multi-resolution analysis with deep learning in a CNN-based framework, differing significantly from prior approaches.
PET	DirectPet [126]	2020	DirectPET introduces an efficient neural network with a Radon inversion layer for fast, high-quality multi-slice PET reconstruction from sinograms.
	DLE [127]	2022	Deep learning-based enhancement improves oncology 18F-FDG PET scan quality, enabling shorter scan and reconstruction times while preserving accuracy.
	Deidda1 et al. [128]	2023	A triple-modality PET/SPECT/CT reconstruction method is proposed to enhance PET image quality, significantly improving lesion uptake quantification for theranostic applications.

*Continued on next page*

Modality	Paper	Year	Detail
	Hashimoto et al. [129]	2023	A shape-aware diffusion model for 3D image reconstruction from limited 2D images, incorporating shape priors to enhance topology.
	Gong et al. [130]	2024	Proposes and evaluates denoising diffusion probabilistic model based methods for PET image denoising, demonstrating that incorporating PET and MRI priors improves performance over traditional denoising approaches.
SPECT	Mostafapour et al. [131]	2022	Using residual and UNet deep convolutional neural networks, it investigates the accuracy of direct attenuation correction in the image domain for myocardial perfusion SPECT imaging.
CT MRI	DiffusionMBIR [132]	2023	Integrates diffusion models with model-based iterative reconstruction to enable efficient and high-fidelity 3D medical image reconstruction from pre-trained 2D diffusion priors.

Table 5: Related works on Gaussian-based radiological image reconstruction.

Modality	Paper	Year	Detail
CT	Li et al. [134]	2023	A self-supervised 3D Gaussian method using FBP priors and adaptive updates for efficient sparse-view CT reconstruction.
	DIF-Gaussian [135]	2024	A framework for sparse-view CBCT reconstruction using 3D Gaussian features and test-time optimization to improve anatomical imaging.
	R <sup>2</sup> -Gaussian [45]	2024	A novel 3D Gaussian splatting framework that rectifies integration bias for rapid, accurate sparse-view tomographic reconstruction.
	GaSpCT [136]	2024	GaSpCT synthesizes CT views from limited 2D images without SfM reducing scan time and enhancing foreground/background separation.
	DDGS-CT [137]	2024	A direction-disentangled 3D Gaussian splatting framework for efficient, differentiable DRR generation modeling anisotropic X-ray effects for intraoperative imaging.
	X-Gaussian [138]	2025	A 3D Gaussian splatting-based framework for efficient, high-quality novel X-ray view synthesis and rapid sparse-view CT reconstruction.
CT MRI	GBIR [139]	2025	A Gaussian-Based Iterative Reconstruction framework that leverages learnable Gaussians for personalized CT and MRI reconstruction from undersampled data, overcoming deep learning limitations and validated on the MORE dataset.

## 5. Implicit reconstruction methods

Unlike discrete explicit representations that directly encode features or signal values, implicit representations are defined as continuous generative functions that map input coordinates to corresponding values within the input space [39]. Existing implicit representations in radiology imaging applications can be categorized into two main types: Implicit Prior Embedding (IPE) and Neural Radiance Fields (NRF). IPE incorporates prior information into the representation space or model parameter space, allowing the

model to automatically learn features that conform to the given prior during training. This approach has been applied to various imaging modalities, including CT [156], PET [157, 158], and multi-modality [159, 160] applications. For a literature review on implicit prior embedding, refer to Table 6. On the other hand, NRF have gained attention in radiology imaging reconstruction since their introduction due to their ability to generate high-resolution, photorealistic images and render realistic 3D views from arbitrary perspectives [40]. NRFs have been applied to US [88, 161, 162, 163], CT [164, 41, 135, 165, 166, 167, 168], MRI [169, 170], and multi-modality [171, 172, 173] imaging. The literature review on the NRF method can be found in Table 7. Next, we will discuss representative papers for each method.

### 5.1. Implicit Prior Embedding

Unlike previous explicit prior embeddings, implicit prior embedding is an implicit neural representation learning methodology that reconstructs radiological images by integrating prior image information into the neural network architecture [159].

Initially, this approach was applied in PET imaging to reconstruct normal-dose images from low-dose scans. For instance, Gong et al. integrated the deep image prior framework with a nonlocal operation, using a kernel matrix layer for feature denoising and embedding linear kinetic models as convolutional layers [157]. Experimental results demonstrated better performance compared to traditional methods and kernel-based approaches [157]. This approach enhances parametric image reconstruction, improving image quality and reducing noise.

Subsequently, NeRP [159] extended this methodology to multi-modality imaging, pioneering a unified framework for medical image reconstruction. It captures subtle yet significant image changes required for assessing tumor progression, thereby improving reconstruction quality. Unlike previous methods, NeRP employs an implicit neural network to directly learn a continuous representation of the target image, eliminating the need for explicit pixel storage. Additionally, it integrates prior embedding mechanisms, enabling the model to effectively extract structural information and optimize the reconstruction process in conjunction with physical measurements. By using an MLP to map spatial coordinates to intensity values, NeRP has demonstrated superior performance in reconstructing CT and MRI images. It achieved a PSNR of 39.06 dB and an SSIM of 0.986 using just 20 projections, outperforming other methods like FBP and GRFF [159].

Numerous studies [174, 160, 159, 156] have demonstrated that implicit prior embedding can effectively ensure high-quality radiological image reconstruction, particularly in converting low-dose images to normal-dose ones. However, this approach has significant limitations. Firstly, it requires each subject to undergo at least one normal-dose scan, significantly restricting its applicability [159]. Moreover, in real-world scenarios, prior images may not always be available due to anatomical variations, patient movement, or differences between imaging devices, making perfect alignment with the target image difficult [175].

### 5.2. Neural Radiance Fields

Neural Radiance Fields (NeRF) have emerged as a powerful technique for 3D reconstruction and rendering. Unlike traditional methods that depend on discrete volume representations, NeRF offers enhanced performance in generating detailed medical images [40, 167] delivering high-quality results in medical imaging, especially for CT reconstruction.

MedNeRF [41] was the first to apply NeRF to radiological imaging. It employs self-supervised learning and extends the Generative Radiance Field (GRAF) framework with a GAN architecture tailored for the medical domain. This approach combines self-supervised learning and data augmentation techniques to enhance the fidelity of reconstructions from sparse data [41]. Trained and validated on Digital Reconstructed Radiographs (DRRs), MedNeRF demonstrated high-quality rendering when reconstructing from single-view X-rays, achieving a PSNR of 30.17 dB and an SSIM of 0.670. However, this method heavily relies on single-view X-ray for CT reconstruction, resulting in significant artifacts in the visualized reconstruction, limiting its clinical application.

VolumeNeRF [167] employs a 3D encoder-decoder architecture to reconstruct CT volumes from 2D X-rays, incorporating anatomical priors from likelihood and average CT images. A projection attention module enhances spatial alignment, while Lambert-Beer law-based volumetric rendering synthesizes X-rays for additional supervision. This method improves reconstruction quality, preserving edges and anatomical details.

When applied to ultrasound imaging, a notable pioneering method is Ultra-NeRF [88], an innovative implicit neural representation (INR) model for ultrasound (US) imaging that synthesizes view-dependent B-mode images from multiple 2D ultrasound scans. Ultra-NeRF incorporates physics-based rendering formulas and employs ray tracing to account for the anisotropic

properties of ultrasound, such as tissue-specific attenuation, reflection, and scattering. This allows for accurate synthesis of new perspectives of the 3D anatomical structure. Ultra-NeRF outperforms baseline INR models without rendering, capturing view-dependent phenomena such as acoustic shadowing and occlusions. Its qualitative comparison with volumetric synthesis also shows significant advantages.

Following this, Chen et al. [172] introduced CuNeRF, a zero-shot framework for applying NeRF across radiological imaging modalities, both CT and MRI. It reconstructs high-resolution medical volumes from low-resolution inputs without paired HR data, using cubic grids for sampling, isotropic volume rendering, and hierarchical adaptive sampling. CuNeRF outperformed SOTA methods, achieving a PSNR of 39.62 dB and SSIM of 0.9786 at 2 scale on the MSD dataset, while enabling free-viewpoint synthesis and robust performance across settings.

NeRF-based radiological image reconstruction methods have gained widespread attention in recent years. However, computational complexity remains a significant barrier to their clinical application [39]. These methods require learning a neural representation for each signal individually, which demands substantial memory and computational resources. This challenge is especially pronounced when processing high-dimensional data, such as 3D volumes, resulting in a time-consuming training process. Additionally, implicit reconstruction is prone to image blurring and structural distortion due to sparse sampling, which can be critical in medical imaging.

Table 6: Related works on implicit-prior-based radiological image reconstruction.

Modality	Paper	Year	Detail
CT	PINER [156]	2023	A novel source-free black-box test-time adaptation approach via prior-informed implicit neural representation learning for sparse-view CT reconstruction with unknown noise levels.
PET	GONG et al. [157]	2022	An unsupervised deep learning framework for dynamic PET parametric reconstruction, using 3D U-Net with embedded kinetic model as a convolution layer.
	Makkar et al. [158]	2024	A deep learning-based approach enhances image quality in partial-ring PET scanners using implicit neural representation learning with coordinate-based MLPs.
CT MRI	NeRP [159]	2022	An implicit neural representation learning methodology integrating longitudinal information into deep learning models with anatomical information as the image prior for reconstructing computational images from sparse measurements.

*Continued on next page*

Modality	Paper	Year	Detail
	Liu et al. [160]	2025	A geometry-aware encoder-decoder framework for sparse use-view CBCT reconstruction by leveraging the prior knowledge and back-projecting multiview 2D features into 3D space.

Table 7: Related works on NeRF-based radiological image reconstruction.

Modality	Paper	Year	Detail
US	Ultra-NeRF [88]	2023	A ray-tracing-based method for synthesizing accurate B-mode images by learning view-dependent scene appearance and geometry from multiple US sweeps.
	UIRe-NeRF [161]	2024	A ultrasound neural rendering model integrating implicit neural networks and explicit volume rendering, featuring reflection direction parameterization and harmonic encoding.
	NeRF-US [162]	2024	An approach for training NeRFs on ultrasound imaging that incorporates the properties of ultrasound imaging and incorporates 3D priors through a diffusion model, also utilizing ultrasound-specific rendering.
	ImplicitVol [163]	2021	A model for deep implicit 3D volume sensorless reconstruction from 2D freehand ultrasound images, featuring implicit spatial-to-intensity mapping.
CT	MedNeRF [41]	2022	A novel NeRF-based deep learning architecture for continuous CT scan representation from a few single-view X-ray.
	NAF [164]	2022	NAF advances self-supervised sparse-view CBCT reconstruction without external training data.
	DIF-Net [176]	2023	A supervised CBCT reconstruction framework for high-quality, high-resolution CBCT from $\leq 10$ sparse views.
	ACnerf [165]	2024	ACnerf improves NeRF-based single-view X-ray CT reconstruction by enhancing alignment, pose correction, and rendering precision.
	UMedNeRF [166]	2024	A radiance field-based network for continuous CT projection representation from 2D X-rays, with internal structure extraction and multi-task loss optimization.
	VolumeNeRF [167]	2024	VolumeNeRF reconstructs CT volumes from a single-view X-ray using NeRF with anatomical priors and a projection attention module.
	SAX-NeRF [168]	2024	SAX-NeRF improves sparse-view X-ray 3D reconstruction by introducing Lineformer for structural modeling and Masked Local-Global ray sampling for enhanced feature extraction.
MRI	extended-MedNeRF [169]	2023	A neural radiance field-based approach for reconstructing 3D projections from 2D MRI slices.
	Feng et al. [170]	2025	An INR-based unsupervised deep learning approach that reconstructs dynamic MRI from highly undersampled k-space data using only spatiotemporal coordinate inputs.
CT MRI	NeSVoR [171]	2023	A resolution-agnostic slice-to-volume reconstruction framework that represents the underlying volume as a continuous spatial function using implicit neural representation.
	CuNeRF [172]	2023	A zero-shot medical image super-resolution framework that generates high-quality images at arbitrary scales and viewpoints without requiring high-resolution training data.

*Continued on next page*

Modality	Paper	Year	Detail
	RAO et al. [173]	2022	An energy-efficient accelerator with co-designed hardware architecture for Implicit Neural Representation (INR)-based medical image reconstruction, optimizing both data reuse patterns and computational load distribution.

## 6. Challenges and Opportunities

### 6.1. Imaging Quality

With AI advancing 3D reconstruction in radiological imaging, methods have evolved from slice-based (4.1) to volume-based (4.2), Gaussian representation (4.3), and implicit-based (5) techniques, continuously improving metrics like PSNR and SSIM [177]. However, medical imaging quality assessment must go beyond computational benchmarks to consider clinical relevance [178], including artifacts [179], registration accuracy [180], and fidelity [181]. Clinician evaluation remains essential in complementing these metrics.

In the field of natural image quality assessment, numerous studies have demonstrated that combining Image Quality Assessment (IQA) [182] with Image Quality Metrics (IQM) [183] that is, integrating comprehensive survey evaluations with mathematical metrics provides a more effective means of assessing image quality. This approach is particularly prevalent in image restoration tasks such as deblurring [184] and low-light enhancement [185, 186, 187, 188, 189].

Similarly, some attempts have been made in the medical field [190, 191, 192]. We believe that extensive medical clinical evaluations hold greater practical value than achieving high metric scores.

At the same time, the adoption of more diverse and effective evaluation metrics can further enhance reconstruction quality [193]. Whether in natural images or medical imaging, selecting appropriate evaluation metrics can help guide models to learn deeper and more meaningful information [194, 195].

### 6.2. Efficiency & Effectiveness

Early convolutional neural networks enabled fast but basic reconstruction (4.1), while advanced models such as diffusion models (4.2) and NeRF (5.2) struggle with the trade-off between quality and speed. 3DGS (4.3) addresses this issue by leveraging Gaussian representations and parallel computing for



fast, high-fidelity reconstruction. However, achieving both rapid and high-quality results remains a key AI research focus in medical imaging [196, 197].

Transfer learning, which involves pretraining models on large-scale datasets and fine-tuning them for specific medical imaging tasks, effectively reduces training time and computational costs [198]. In the medical field, transfer learning has been widely applied to classification [199], segmentation [200], and other tasks [201]. Notably, the emergence of Segment Anything Model (SAM) [202] has demonstrated precise medical image segmentation through fine-tuning [203]. Unlike classification and segmentation, radiological image reconstruction relies on the unique attributes of medical images, making direct application challenging [204, 205]. Instead, embedding imaging-specific knowledge is essential for achieving optimal results.

Another promising approach is edge computing, which offloads computationally intensive tasks to edge devices or cloud platforms, enabling real-time and distributed AI processing [206]. In large language models, edge computing has been widely adopted [207]. In the field of radiological image reconstruction, Isosalo et al. [208] have explored the feasibility of local edge computing for radiological image reconstruction and computer-aided detection. Zhang et al. [209] utilized edge computing in IoT-based 3D telemedicine for denoising CT images. Additionally, Zhang et al. [210] proposed a collaborative inference strategy for medical image diagnosis in a mobile edge computing environment. We believe that integrating radiological image reconstruction with edge computing holds great clinical value, offering potential solutions for real-time imaging.

Meanwhile, advancements in AI-driven low-dose and sparse-view reconstruction have reduced medical imaging costs, though the primary expense now lies in the computational resources required for high-performance AI models. To further reduce costs, developing lightweight end-to-end models with fewer parameters is crucial. Additionally, knowledge distillation has emerged as a popular solution [211]. In medical segmentation, Zhou et al. [212] proposed a one-shot medical image segmentation framework based on image reconstruction-guided distillation learning, effectively reducing computational demands. In the context of medical imaging reconstruction, Wu et al. [213] introduced an unsupervised MRI reconstruction method based on self-supervised training, knowledge distillation, and sample reweighting. By training a teacher model and distilling its knowledge into a student model, their approach accelerated inference while improving performance across multiple datasets.

### 6.3. Privacy Protection

Given the sensitivity of medical imaging data, secure AI-driven reconstruction is crucial [214]. To address this challenge, numerous solutions have been proposed.

First, various unsupervised models have been developed, incorporating Gaussian mixture models [215], unbiased risk estimation [216], or 3DGS-based [217, 138] architectures. These algorithms operate without requiring training datasets or external patient information [218], providing a promising approach to enhancing patient privacy.

Federated Learning ensures privacy preservation by training models on decentralized data sources without transferring sensitive patient data [219]. This approach has been successfully applied to MRI reconstruction, achieving results that closely match multi-institutional data distributions [220, 221].

Additionally, domain adaptation [222, 223] and domain generalization [224] techniques help mitigate domain shifts between public datasets and clinical data, preventing the need for direct training on clinical datasets. Recently, Test-Time Training has emerged as a focal point in this area [225, 226].

Moreover, integrating differential privacy into AI models ensures that individual data points remain protected during the reconstruction process [227]. The application of homomorphic encryption can further enable computations on encrypted medical data without compromising privacy [228, 229].

Blockchain-based secure data sharing has also gained attention [230], as it ensures the secure and transparent exchange of medical imaging data while safeguarding patient confidentiality [231].

### 6.4. Model Interpretability

The opacity of complex AI-based reconstruction models limits clinical trust [232]. To improve interpretability, recent models decompose reconstruction into traceable steps [233]. Current methods mainly fall into two categories: ante-hoc interpretability [234, 235] and post-hoc interpretability [236, 237].

In the field of radiological image reconstruction, Zhang et al. proposed DUN-SA by unfolding the iterative stages of an optimization algorithm into network modules with clear physical meanings [238]. This approach makes the learning process more interpretable and addresses the lack of explainability in deep learning-based multimodal MRI reconstruction.

We believe that improving the interpretability of radiological image reconstruction models will accelerate the clinical deployment of AI.

## 7. Conclusion

Since the development of computer vision technology in artificial intelligence, its applications in medical imaging analysis have become increasingly widespread. This review primarily examines its applications in 3D reconstruction for radiological imaging, covering multiple imaging modalities, including CT, MRI, PET, SPECT, and US. Over the past five years, there has been a substantial increase in research articles on artificial intelligence-based 3D reconstruction algorithms for radiological imaging.

This review categorizes existing literature into explicit and implicit reconstruction methods based on imaging approaches. It further provides a comprehensive discussion of the development, advantages, and limitations of these two representation paradigms in the field.

Given the unique characteristics of medical imaging, artificial intelligence algorithms must balance multiple factors, including image quality, computational efficiency, and imaging cost. As current algorithmic trends evolve, an increasing number of researchers are expected to propose more efficient reconstruction methods that enhance medical image quality within limited computational time and cost. In the future, artificial intelligence is anticipated to enable low-cost, high-quality medical image reconstruction through end-to-end systems, facilitating rapid and cost-effective imaging solutions.

## References

- [1] D. Sanghvi, M. Harisinghani, Modalities in modern radiology: A synopsis, *Journal of postgraduate medicine* 56 (2) (2010) 85–87.
- [2] D. Shen, G. Wu, H.-I. Suk, Deep learning in medical image analysis, *Annual review of biomedical engineering* 19 (1) (2017) 221–248.
- [3] H. Ben Yedder, B. Cardoen, G. Hamarneh, Deep learning for biomedical image reconstruction: A survey, *Artificial intelligence review* 54 (1) (2021) 215–251.
- [4] S. P. Singh, L. Wang, S. Gupta, H. Goli, P. Padmanabhan, B. Gulyás, 3d deep learning on medical images: a review, *Sensors* 20 (18) (2020) 5097.
- [5] J. M. Blackledge, *Digital image processing: mathematical and computational methods*, Elsevier, 2005.
- [6] R. Gothwal, S. Tiwari, S. Shivani, Computational medical image reconstruction techniques: a comprehensive review, *Archives of Computational Methods in Engineering* 29 (7) (2022) 5635–5662.

- [7] H. Shi, S. Luo, Z. Yang, G. Wu, A novel iterative ct reconstruction approach based on fbp algorithm, *PLoS one* 10 (9) (2015) e0138498.
- [8] J. W. Cooley, P. A. Lewis, P. D. Welch, The fast fourier transform and its applications, *IEEE Transactions on Education* 12 (1) (1969) 27–34.
- [9] T. Sumanaweera, D. Liu, Medical image reconstruction with the fft, *GPU gems* 2 (2005) 765–784.
- [10] K. H. Jin, M. T. McCann, E. Froustey, M. Unser, Deep convolutional neural network for inverse problems in imaging, *IEEE transactions on image processing* 26 (9) (2017) 4509–4522.
- [11] J. A. Fessler, Medical image reconstruction: a brief overview of past milestones and future directions, *arXiv preprint arXiv:1707.05927* (2017).
- [12] R. Gordon, R. Bender, G. T. Herman, Algebraic reconstruction techniques (art) for three-dimensional electron microscopy and x-ray photography, *Journal of theoretical Biology* 29 (3) (1970) 471–481.
- [13] S. Ravishankar, J. C. Ye, J. A. Fessler, Image reconstruction: From sparsity to data-adaptive methods and machine learning, *Proceedings of the IEEE* 108 (1) (2019) 86–109.
- [14] H. M. Hudson, R. S. Larkin, Accelerated image reconstruction using ordered subsets of projection data, *IEEE transactions on medical imaging* 13 (4) (1994) 601–609.
- [15] R. Yao, J. Seidel, C. A. Johnson, M. E. Daube-Witherspoon, M. V. Green, R. E. Carson, Performance characteristics of the 3-d osem algorithm in the reconstruction of small animal pet images, *IEEE transactions on medical imaging* 19 (8) (2000) 798–804.
- [16] E. Rapisarda, V. Bettinardi, K. Thielemans, M. Gilardi, Image-based point spread function implementation in a fully 3d osem reconstruction algorithm for pet, *Physics in medicine & biology* 55 (14) (2010) 4131.
- [17] Y. Vardi, L. A. Shepp, L. Kaufman, A statistical model for positron emission tomography, *Journal of the American statistical Association* 80 (389) (1985) 8–20.
- [18] G. Wang, J. C. Ye, B. De Man, Deep learning for tomographic image reconstruction, *Nature machine intelligence* 2 (12) (2020) 737–748.
- [19] A. Subasi, Artificial intelligence for 3d medical image analysis, in: *Applications of Artificial Intelligence Healthcare and Biomedicine*, Elsevier, 2024, pp. 357–375.
- [20] A. Hosny, C. Parmar, J. Quackenbush, L. H. Schwartz, H. J. Aerts, Artificial intelligence in radiology, *Nature Reviews Cancer* 18 (8) (2018) 500–510.
- [21] S. Wang, R. M. Summers, Machine learning and radiology, *Medical image analysis* 16 (5) (2012) 933–951.
- [22] Y. LeCun, B. Boser, J. S. Denker, D. Henderson, R. E. Howard, W. Hubbard, L. D. Jackel, Back-propagation applied to handwritten zip code recognition, *Neural computation* 1 (4) (1989) 541–551.
- [23] C. Chen, N. A. M. Isa, X. Liu, A review of convolutional neural network based methods for medical image classification, *Computers in Biology and Medicine* 185 (2025) 109507.
- [24] J. Jurek, M. Kociński, A. Materka, M. Elgalal, A. Majos, Cnn-based superresolution reconstruction of 3d mr images using thick-slice scans, *Biocybernetics and Biomedical Engineering* 40 (1) (2020) 111–125.

- [25] K. Gong, J. Guan, K. Kim, X. Zhang, J. Yang, Y. Seo, G. El Fakhri, J. Qi, Q. Li, Iterative pet image reconstruction using convolutional neural network representation, *IEEE transactions on medical imaging* 38 (3) (2018) 675–685.
- [26] L. Alzubaidi, J. Zhang, A. J. Humaidi, A. Al-Dujaili, Y. Duan, O. Al-Shamma, J. Santamaría, M. A. Fadhel, M. Al-Amidie, L. Farhan, Review of deep learning: concepts, cnn architectures, challenges, applications, future directions, *Journal of big Data* 8 (2021) 1–74.
- [27] A. Waswani, N. Shazeer, N. Parmar, J. Uszkoreit, L. Jones, A. Gomez, L. Kaiser, I. Polosukhin, Attention is all you need, in: *NIPS*, 2017.
- [28] A. Dosovitskiy, L. Beyer, A. Kolesnikov, D. Weissenborn, X. Zhai, T. Unterthiner, M. Dehghani, M. Minderer, G. Heigold, S. Gelly, et al., An image is worth 16x16 words: Transformers for image recognition at scale, *arXiv preprint arXiv:2010.11929* (2020).
- [29] R. Azad, A. Kazerouni, M. Heidari, E. K. Aghdam, A. Molaei, Y. Jia, A. Jose, R. Roy, D. Merhof, Advances in medical image analysis with vision transformers: a comprehensive review, *Medical Image Analysis* 91 (2024) 103000.
- [30] A. M. Ali, B. Benjdira, A. Koubaa, W. El-Shafai, Z. Khan, W. Boulila, Vision transformers in image restoration: A survey, *Sensors* 23 (5) (2023) 2385.
- [31] D. P. Kingma, M. Welling, et al., Auto-encoding variational bayes (2013).
- [32] I. Goodfellow, J. Pouget-Abadie, M. Mirza, B. Xu, D. Warde-Farley, S. Ozair, A. Courville, Y. Bengio, Generative adversarial nets, *Advances in neural information processing systems* 27 (2014).
- [33] Y. Luo, Y. Wang, C. Zu, B. Zhan, X. Wu, J. Zhou, D. Shen, L. Zhou, 3d transformer-gan for high-quality pet reconstruction, in: *Medical Image Computing and Computer Assisted Intervention—MICCAI 2021: 24th International Conference, Strasbourg, France, September 27–October 1, 2021, Proceedings, Part VI* 24, Springer, 2021, pp. 276–285.
- [34] A. Sriram, A. Vatsa, A. Kumar, S. Vats, A. Kumar, Challenges and opportunities in malignant image reconstruction using gan: A review, in: *2024 IEEE Integrated STEM Education Conference (ISEC)*, IEEE, 2024, pp. 01–06.
- [35] F.-A. Croitoru, V. Hondru, R. T. Ionescu, M. Shah, Diffusion models in vision: A survey, *IEEE Transactions on Pattern Analysis and Machine Intelligence* 45 (9) (2023) 10850–10869.
- [36] G. Webber, A. J. Reader, Diffusion models for medical image reconstruction, *BJR— Artificial Intelligence* 1 (1) (2024) ubae013.
- [37] A. Güngör, S. U. Dar, Ş. Öztürk, Y. Korkmaz, H. A. Bedel, G. Elmas, M. Ozbey, T. Çukur, Adaptive diffusion priors for accelerated mri reconstruction, *Medical image analysis* 88 (2023) 102872.
- [38] M. Chen, S. Mei, J. Fan, M. Wang, Opportunities and challenges of diffusion models for generative ai, *National Science Review* 11 (12) (2024) nwae348.
- [39] A. Molaei, A. Aminimehr, A. Tavakoli, A. Kazerouni, B. Azad, R. Azad, D. Merhof, Implicit neural representation in medical imaging: A comparative survey, in: *Proceedings of the IEEE/CVF International Conference on Computer Vision*, 2023, pp. 2381–2391.
- [40] B. Mildenhall, P. P. Srinivasan, M. Tancik, J. T. Barron, R. Ramamoorthi, R. Ng, Nerf: Representing scenes as neural radiance fields for view synthesis, *Communications of the ACM* 65 (1) (2021) 99–106.

- [41] A. Corona-Figueroa, J. Frawley, S. Bond-Taylor, S. Bethapudi, H. P. Shum, C. G. Willcocks, Mednerf: Medical neural radiance fields for reconstructing 3d-aware ct-projections from a single x-ray, in: 2022 44th annual international conference of the IEEE engineering in medicine & Biology society (EMBC), IEEE, 2022, pp. 3843–3848.
- [42] X. Wang, S. Hu, H. Fan, H. Zhu, X. Li, Neural radiance fields in medical imaging: Challenges and next steps, arXiv preprint arXiv:2402.17797 (2024).
- [43] B. Kerbl, G. Kopanas, T. Leimkühler, G. Drettakis, 3d gaussian splatting for real-time radiance field rendering., ACM Trans. Graph. 42 (4) (2023) 139–1.
- [44] B. Fei, J. Xu, R. Zhang, Q. Zhou, W. Yang, Y. He, 3d gaussian splatting as new era: A survey, IEEE Transactions on Visualization and Computer Graphics (2024).
- [45] R. Zha, T. J. Lin, Y. Cai, J. Cao, Y. Zhang, H. Li,  $r^2$ -gaussian: Rectifying radiative gaussian splatting for tomographic reconstruction, arXiv preprint arXiv:2405.20693 (2024).
- [46] E. Ahishakiye, M. Bastiaan Van Gijzen, J. Tumwiine, R. Wario, J. Obungoloch, A survey on deep learning in medical image reconstruction, Intelligent Medicine 1 (03) (2021) 118–127.
- [47] M. Yasmin, M. Sharif, S. Masood, M. Raza, S. Mohsin, Brain image reconstruction: A short survey, World Applied Sciences Journal 19 (1) (2012) 52–62.
- [48] Web of science.  
URL <https://www.webofscience.com/>
- [49] Google scholar.  
URL <https://scholar.google.com/>
- [50] Scopus.  
URL <https://www.scopus.com/>
- [51] M. Sarmah, A. Neelima, H. R. Singh, Survey of methods and principles in three-dimensional reconstruction from two-dimensional medical images, Visual computing for industry, biomedicine, and art 6 (1) (2023) 15.
- [52] J. Li, G. Zhu, C. Hua, M. Feng, B. Bennamoun, P. Li, X. Lu, J. Song, P. Shen, X. Xu, et al., A systematic collection of medical image datasets for deep learning, ACM Computing Surveys 56 (5) (2023) 1–51.
- [53] J. Ogier du Terrail, S.-S. Ayed, E. Cyffers, F. Grimberg, C. He, R. Loeb, P. Mangold, T. Marchand, O. Marfoq, E. Mushtaq, et al., Flamby: Datasets and benchmarks for cross-silo federated learning in realistic healthcare settings, Advances in Neural Information Processing Systems 35 (2022) 5315–5334.
- [54] J. Kulynych, H. T. Greely, Clinical genomics, big data, and electronic medical records: reconciling patient rights with research when privacy and science collide, Journal of Law and the Biosciences 4 (1) (2017) 94–132.
- [55] M. T. Löffler, A. Sekuboyina, A. Jacob, A.-L. Grau, A. Scharr, M. El Hussein, M. Kallweit, C. Zimmer, T. Baum, J. S. Kirschke, A vertebral segmentation dataset with fracture grading, Radiology: Artificial Intelligence 2 (4) (2020) e190138.
- [56] A. Sekuboyina, M. E. Hussein, A. Bayat, M. Löffler, H. Liebl, H. Li, G. Tetteh, J. Kukačka, C. Payer, D. Štern, et al., Verse: a vertebrae labelling and segmentation benchmark for multi-detector ct images, Medical image analysis 73 (2021) 102166.

- [57] H. Liebl, D. Schinz, A. Sekuboyina, L. Malagutti, M. T. Löffler, A. Bayat, M. El Hussein, G. Tetteh, K. Grau, E. Niederreiter, et al., A computed tomography vertebral segmentation dataset with anatomical variations and multi-vendor scanner data, *Scientific data* 8 (1) (2021) 284.
- [58] S. G. Armato III, G. McLennan, L. Bidaut, M. F. McNitt-Gray, C. R. Meyer, A. P. Reeves, B. Zhao, D. R. Aberle, C. I. Henschke, E. A. Hoffman, et al., The lung image database consortium (lidc) and image database resource initiative (idri): a completed reference database of lung nodules on ct scans, *Medical physics* 38 (2) (2011) 915–931.
- [59] J. Zhao, Y. Zhang, X. He, P. Xie, Covid-ct-dataset: A CT scan dataset about COVID-19, *CoRR abs/2003.13865* (2020). [arXiv:2003.13865](https://arxiv.org/abs/2003.13865).  
URL <https://arxiv.org/abs/2003.13865>
- [60] R. Castillo, E. Castillo, R. Guerra, V. E. Johnson, T. McPhail, A. K. Garg, T. Guerrero, A framework for evaluation of deformable image registration spatial accuracy using large landmark point sets, *Physics in Medicine & Biology* 54 (7) (2009) 1849.
- [61] N. Heller, N. Sathianathan, A. Kalapara, E. Walczak, K. Moore, H. Kaluzniak, J. Rosenberg, P. Blake, Z. Rengel, M. Oestreich, et al., The kits19 challenge data: 300 kidney tumor cases with clinical context, ct semantic segmentations, and surgical outcomes, *arXiv preprint arXiv:1904.00445* (2019).
- [62] T. R. Moen, B. Chen, D. R. Holmes III, X. Duan, Z. Yu, L. Yu, S. Leng, J. G. Fletcher, C. H. McCollough, Low-dose ct image and projection dataset, *Medical physics* 48 (2) (2021) 902–911.
- [63] Y. Deng, C. Wang, Y. Hui, Q. Li, J. Li, S. Luo, M. Sun, Q. Quan, S. Yang, Y. Hao, et al., Ctspine1k: a large-scale dataset for spinal vertebrae segmentation in computed tomography, *arXiv preprint arXiv:2105.14711* (2021).
- [64] E. B. Tsai, S. Simpson, M. P. Lungren, M. Hershman, L. Roshkovan, E. Colak, B. J. Erickson, G. Shih, A. Stein, J. Kalpathy-Cramer, J. Shen, M. A. F. Hafez, S. John, P. Rajiah, B. P. Pogatchnik, J. T. Mongan, E. Altinmakas, E. Ranschaert, F. C. Kitamura, C. Wu, Medical imaging data resource center (midrc) - rsna international covid open research database (ricord) release 1b - chest ct covid- (version 1) [data set] (2021).  
URL <https://doi.org/10.7937/31V8-4A40>
- [65] S. Bakas, C. Carr, A. Flanders, J. Kalpathy-Cramer, J. Mongan, B. Menze, L. M. Prevedello, Rsna-miccai brain tumor segmentation (brats) challenge 2021 (Mar. 2021). [doi:10.5281/zenodo.4575162](https://doi.org/10.5281/zenodo.4575162).
- [66] M. Aboian, U. Anazodo, U. Baid, S. Bakas, E. Calabrese, G. Marco Conte, A. Kazerooni, Y. Kirchhoff, F. Kofler, D. LaBella, H. Li, M. G. Linguraru, B. Menze, J. Rudie, P. Vollmuth, B. Wiestler, Miccai 2025 lighthouse challenge: Brain tumor segmentation cluster of challenges (brats) (Oct. 2024). [doi:10.5281/zenodo.13981216](https://doi.org/10.5281/zenodo.13981216).
- [67] S. Bakas, U. Baid, K. Farahani, J. Albrecht, J. Eddy, T. Bergquist, T. Yu, V. Chung, R. T. Shinohara, M. Bilello, S. Mohan, S. Ghodasara, A. W. Moawad, J. Rudie, L. O. Coelho, E. Miller, F. E. Morn, M. C. Oswood, R. Y. Shih, L. Siakallis, Y. Bronstein, J. R. Mason, A. F. Miller, G. Choudhary, A. Agarwal, C. H. Besada, J. J. Derakhshan, M. C. Diogo, D. D. Do-Dai, L. Farage, J. L. Go, M. Hadi, V. B. Hill, M. Iv, D. Joyner, C. Lincoln, E. Lotan, A. Miyakoshi, M. Sanchez-Montao, J. Nath, X. V. Nguyen, M. Nicolas-Jilwan, J. O. Jimenez, K. Ozturk, B. D. Petrovic, L. M. Shah, C. Shah, M. Sharma, O. Simsek, A. K. Singh, V. Statsevych, B. D. Weinberg, R. J. Young, I. Ikuta, A. K. Agarwal, S. C. Cambron, R. Silbergleit, A. Dusoi, A. A. Postma, L. Letourneau-Guillon, G. J. G. Prez-Carrillo, A. Saha, N. Soni, G. Zaharchuk, V. M. Zohrabian, Y. Chen, M. M. Cekic, A. Rahman, J. E. Small, V. Sethi, C. Davatzikos, J. Mongan, E. Calabrese, C. Hess, S. Cha, J. Villanueva-Meyer, J. B. Freymann, J. S. Kirby, B. Menze, E. Colak, P. Crivella, R. R. Colen, A. Kotrotsou, D. Marcus, M. Milchenko, A. Nazeri, H. Fathallah-Shayk, R. Wiest, A. Jakab, M.-A. Weber, A. Mahajan, U. Anazodo, M. Adewole, F. Dako, O. Toyobo, A. Mintz,

- O. Omidiji, K. Iorpagher, Y. Gbadamosi, A. Ogunleye, N. Ojo, E. Ofeimun, U. Douglas, G. Babatunde, K. Aguh, A. Emegoakor, M. Nwabunike, W. Wiggins, Z. Reitman, C. Wang, D. LaBella, G. Khanna, J. Villanueva-Meyer, J. Kirkpatrick, M. Aboian, S. A. Fadel, A. Janas, M. G. Linguraru, A. F. Kazerooni, X. Liu, Z. Jiang, A. Familiar, A. Vossough, M. Bornhorst, A. Nabavizadeh, N. Lepore, J. Palmer, A. Porras, K. Swanson, H. B. Li, B. Wiestler, J. E. Iglesias, S. M. Anwar, K. V. Leemput, F. Kofler, C. Bukas, M. Piraud, G. M. Conte, O. McDonnell, S. Soman, E. Johanson, Z. Meier, The international brain tumor segmentation (brats) cluster of challenges (Apr. 2023). doi:10.5281/zenodo.7837974.
- [68] S. Bakas, U. Baid, J. Rudie, E. Calabrese, M. Aboian, U. Anazodo, G. M. Conte, J. Albrecht, H. B. Li, F. Kofler, M. Correia De Verdier, R. Huang, D. LaBella, R. Saluja, L. Gagnon, M. Aboian, A. Abayazeed, K. Farahani, V. Chung, Z. Reitman, J. Kirkpatrick, C. Wang, J. Villanueva-Meyer, A. Flanders, M. Aboian, A. Nada, M. Aboian, A. Abayazeed, P. Lohman, A. Moawad, A. Janas, K. Krantchev, F. Memon, Y. Velichko, E. Schrickel, K. Link, S. Aneja, R. Maresca, A. Nada, P. Vollmuth, V. M. Prez, M. W. Pease, D. Godfrey, S. Floyd, M. Adewole, F. Dako, O. Toyobo, O. Omidiji, Y. Gbadamosi, A. Ogunleye, N. Ojo, K. Iorpagher, G. Babatunde, K. Aguh, A. Emegoakor, C. Kalaiwo, M. G. Linguraru, A. F. Kazerooni, Z. Jiang, X. Liu, D. Gandhi, N. Khalili, A. Vossough, A. Nabavizadeh, J. B. Ware, B. Menze, E. Johanson, Z. Meier, W. Chen, N. Petrick, B. Sahiner, R. Chai, B. Wiestler, J. E. Iglesias, S. M. Anwar, K. Van Leemput, M. Piraud, Brats 2024 cluster of challenges (brats + beyond- brats) (Apr. 2024). doi:10.5281/zenodo.10978907.
- [69] S. Bakas, K. Farahani, M. G. Linguraru, U. Anazodo, C. Carr, A. Flanders, L. M. Prevedello, F. C. Kitamura, J. Kalpathy-Cramer, J. Mongan, U. Baid, E. Calabrese, J. D. Rudie, E. Colak, Z. Jiang, X. Liu, J. Eddy, T. Bergquist, T. Yu, V. Chung, R. T. Shinohara, A. F. Kazerooni, B. Menze, The brain tumor segmentation challenge (2022 continuous updates & generalizability assessment) (Mar. 2022). doi:10.5281/zenodo.6362180.
- [70] S. Bakas, B. Menze, C. Davatzikos, J. Kalpathy-Cramer, K. Farahani, M. Bilello, S. Mohan, J. B. Freymann, J. S. Kirby, M. Ahluwalia, V. Statsevych, R. Huang, H. Fathallah-Shaykh, R. Wiest, A. Jakab, R. R. Colen, A. Kotrotsou, D. Marcus, M. Milchenko, A. Nazeri, M.-A. Weber, A. Mahajan, U. Baid, Miccai brain tumor segmentation (brats) 2020 benchmark: "prediction of survival and pseudoprogression" (Mar. 2020). doi:10.5281/zenodo.3718904.
- [71] M.-I. Georgescu, R. T. Ionescu, A.-I. Miron, O. Savencu, N.-C. Ristea, N. Verga, F. S. Khan, Multimodal multi-head convolutional attention with various kernel sizes for medical image super-resolution, in: Proceedings of the IEEE/CVF winter conference on applications of computer vision, 2023, pp. 2195–2205.
- [72] C. R. Jack Jr, M. A. Bernstein, N. C. Fox, P. Thompson, G. Alexander, D. Harvey, B. Borowski, P. J. Britson, J. L. Whitwell, C. Ward, et al., The alzheimer's disease neuroimaging initiative (adni): Mri methods, *Journal of Magnetic Resonance Imaging: An Official Journal of the International Society for Magnetic Resonance in Medicine* 27 (4) (2008) 685–691.
- [73] D. S. Marcus, T. H. Wang, J. Parker, J. G. Csernansky, J. C. Morris, R. L. Buckner, Open access series of imaging studies (oasis): cross-sectional mri data in young, middle aged, nondemented, and demented older adults, *Journal of cognitive neuroscience* 19 (9) (2007) 1498–1507.
- [74] F. Knoll, J. Zbontar, A. Sriram, M. J. Muckley, M. Bruno, A. Defazio, M. Parente, K. J. Geras, J. Katsnelson, H. Chandarana, et al., fastmri: A publicly available raw k-space and dicom dataset of knee images for accelerated mr image reconstruction using machine learning, *Radiology: Artificial Intelligence* 2 (1) (2020) e190007.
- [75] J. Zbontar, F. Knoll, A. Sriram, T. Murrell, Z. Huang, M. J. Muckley, A. Defazio, R. Stern, P. Johnson, M. Bruno, et al., fastmri: An open dataset and benchmarks for accelerated mri, *arXiv preprint arXiv:1811.08839* (2018).



- [76] D. C. Van Essen, S. M. Smith, D. M. Barch, T. E. Behrens, E. Yacoub, K. Ugurbil, W.-M. H. Consortium, et al., The wu-minn human connectome project: an overview, *Neuroimage* 80 (2013) 62–79.
- [77] B. A. Landman, A. J. Huang, A. Gifford, D. S. Vikram, I. A. L. Lim, J. A. Farrell, J. A. Bogovic, J. Hua, M. Chen, S. Jarso, et al., Multi-parametric neuroimaging reproducibility: a 3-t resource study, *Neuroimage* 54 (4) (2011) 2854–2866.
- [78] K. Payette, P. de Dumast, H. Kebiri, I. Ezhov, J. C. Paetzold, S. Shit, A. Iqbal, R. Khan, R. Kottke, P. Grethen, et al., An automatic multi-tissue human fetal brain segmentation benchmark using the fetal tissue annotation dataset, *Scientific data* 8 (1) (2021) 167.
- [79] J. Xu, E. Abaci Turk, P. E. Grant, P. Golland, E. Adalsteinsson, Stress: Super-resolution for dynamic fetal mri using self-supervised learning, in: *Medical Image Computing and Computer Assisted Intervention–MICCAI 2021: 24th International Conference, Strasbourg, France, September 27–October 1, 2021, Proceedings, Part VII* 24, Springer, 2021, pp. 197–206.
- [80] E. J. Hughes, T. Winchman, F. Padormo, R. Teixeira, J. Wurie, M. Sharma, M. Fox, J. Hutter, L. Cordero-Grande, A. N. Price, et al., A dedicated neonatal brain imaging system, *Magnetic resonance in medicine* 78 (2) (2017) 794–804.
- [81] A. L. Simpson, M. Antonelli, S. Bakas, M. Bilello, K. Farahani, B. Van Ginneken, A. Kopp-Schneider, B. A. Landman, G. Litjens, B. Menze, et al., A large annotated medical image dataset for the development and evaluation of segmentation algorithms, *arXiv preprint arXiv:1902.09063* (2019).
- [82] X. Zhao, Y. Liao, J. Xie, X. He, S. Zhang, G. Wang, J. Fang, H. Lu, J. Yu, Breastdm: A dce-mri dataset for breast tumor image segmentation and classification, *Computers in Biology and Medicine* 164 (2023) 107255.
- [83] C. Chen, Y. Liu, P. Schniter, M. Tong, K. Zareba, O. Simonetti, L. Potter, R. Ahmad, Ocmr (v1. 0)—open-access multi-coil k-space dataset for cardiovascular magnetic resonance imaging, *arXiv preprint arXiv:2008.03410* (2020).
- [84] A. D. Desai, A. M. Schmidt, E. B. Rubin, C. M. Sandino, M. S. Black, V. Mazzoli, K. J. Stevens, R. Boutin, C. Ré, G. E. Gold, et al., Skm-tea: A dataset for accelerated mri reconstruction with dense image labels for quantitative clinical evaluation, *arXiv preprint arXiv:2203.06823* (2022).
- [85] B. Aubert-Broche, M. Griffin, G. B. Pike, A. C. Evans, D. L. Collins, Twenty new digital brain phantoms for creation of validation image data bases, *IEEE transactions on medical imaging* 25 (11) (2006) 1410–1416.
- [86] C. O. da Costa-Luis, A. J. Reader, Micro-networks for robust mr-guided low count pet imaging, *IEEE transactions on radiation and plasma medical sciences* 5 (2) (2020) 202–212.
- [87] K. Shi, R. Guo, S. Xue, A. Rominger, B. Li, Ultra-low dose pet imaging challenge 2022 (Mar. 2022). doi:10.5281/zenodo.6361846. URL <https://doi.org/10.5281/zenodo.6361846>
- [88] M. Wysocki, M. F. Azampour, C. Eilers, B. Busam, M. Salehi, N. Navab, Ultra-nerf: Neural radiance fields for ultrasound imaging, in: *Medical Imaging with Deep Learning*, PMLR, 2024, pp. 382–401.
- [89] D. Zhao, E. Ferdian, G. D. Maso Talou, G. M. Quill, K. Gilbert, V. Y. Wang, T. P. Babarenda Gamage, J. Pedrosa, J. Dhooge, T. M. Sutton, et al., Mitea: A dataset for machine learning segmentation of the left ventricle in 3d echocardiography using subject-specific labels from cardiac magnetic resonance imaging, *Frontiers in Cardiovascular Medicine* 9 (2023) 1016703.

- [90] A. T. Papageorgiou, E. O. Ohuma, D. G. Altman, T. Todros, L. C. Ismail, A. Lambert, Y. A. Jaffer, E. Bertino, M. G. Gravett, M. Purwar, et al., International standards for fetal growth based on serial ultrasound measurements: the fetal growth longitudinal study of the intergrowth-21st project, *The Lancet* 384 (9946) (2014) 869–879.
- [91] X. Zhuang, L. Li, C. Payer, D. Štern, M. Urschler, M. P. Heinrich, J. Oster, C. Wang, Ö. Smedby, C. Bian, et al., Evaluation of algorithms for multi-modality whole heart segmentation: an open-access grand challenge, *Medical image analysis* 58 (2019) 101537.
- [92] P. J. LaMontagne, S. Keefe, W. Lauren, C. Xiong, E. A. Grant, K. L. Moulder, J. C. Morris, T. L. Benzinger, D. S. Marcus, Ic-p-164: Oasis-3: Longitudinal neuroimaging, clinical, and cognitive dataset for normal aging and alzheimer’s disease, *Alzheimer’s & Dementia* 14 (7S\_Part.2) (2018) P138–P138.
- [93] Z. Baum, S. Saeed, Z. Min, Y. Hu, D. Barratt, Mr to ultrasound registration for prostate challenge-dataset (2023).
- [94] Z. Wang, F. Wang, C. Qin, J. Lyu, C. Ouyang, S. Wang, Y. Li, M. Yu, H. Zhang, K. Guo, et al., Cmrrecon2024: A multimodality, multiview k-space dataset boosting universal machine learning for accelerated cardiac mri, *Radiology: Artificial Intelligence* 7 (2) (2025) e240443.
- [95] B. J. Erickson, F. Kitamura, Magicians corner: 9. performance metrics for machine learning models (2021).
- [96] O. Rainio, J. Teuho, R. Klén, Evaluation metrics and statistical tests for machine learning, *Scientific Reports* 14 (1) (2024) 6086.
- [97] C. Shi, Y. Xiao, Z. Chen, Dual-domain sparse-view ct reconstruction with transformers, *Physica Medica* 101 (2022) 1–7.
- [98] Q. Gao, Z. Li, J. Zhang, Y. Zhang, H. Shan, Corediff: Contextual error-modulated generalized diffusion model for low-dose ct denoising and generalization, *IEEE Transactions on Medical Imaging* (2023).
- [99] J. Du, Z. He, L. Wang, A. Gholipour, Z. Zhou, D. Chen, Y. Jia, Super-resolution reconstruction of single anisotropic 3d mr images using residual convolutional neural network, *Neurocomputing* 392 (2020) 209–220.
- [100] Y. Korkmaz, S. U. H. Dar, M. Yurt, M. zbey, T. ukur, Unsupervised mri reconstruction via zero-shot learned adversarial transformers, *IEEE Transactions on Medical Imaging* 41 (7) (2022) 1747–1763. doi:10.1109/TMI.2022.3147426.
- [101] D. Shen, S. Ghosh, H. Haji-Valizadeh, A. Pathrose, F. Schiffrers, D. C. Lee, B. H. Freed, M. Markl, O. S. Cossairt, A. K. Katsaggelos, et al., Rapid reconstruction of highly undersampled, non-cartesian real-time cine k-space data using a perceptual complex neural network (pcnn), *NMR in Biomedicine* 34 (1) (2021) e4405.
- [102] R. Wei, J. Chen, B. Liang, X. Chen, K. Men, J. Dai, Real-time 3d mri reconstruction from cine-mri using unsupervised network in mri-guided radiotherapy for liver cancer, *Medical Physics* 50 (6) (2023) 3584–3596.
- [103] J. Cui, X. Zeng, P. Zeng, B. Liu, X. Wu, J. Zhou, Y. Wang, Mcad: Multi-modal conditioned adversarial diffusion model for high-quality pet image reconstruction, in: *International Conference on Medical Image Computing and Computer-Assisted Intervention*, Springer, 2024, pp. 467–477.
- [104] Y. Wang, Y. Luo, C. Zu, B. Zhan, Z. Jiao, X. Wu, J. Zhou, D. Shen, L. Zhou, 3d multi-modality transformer-gan for high-quality pet reconstruction, *Medical Image Analysis* 91 (2024) 102983.

- [105] I. R. Singh, A. Denker, R. Barbano, . Kereta, B. Jin, K. Thielemans, P. Maass, S. Arridge, Score-based generative models for pet image reconstruction, *Machine Learning for Biomedical Imaging 2* (2024) 547–585. doi:<https://doi.org/10.59275/j.melba.2024-5d51>. URL <https://melba-journal.org/2024:001>
- [106] F. Yousefzadeh, M. Yazdi, S. M. Entezarmahdi, R. Faghihi, S. Ghasempoor, N. Shahamiri, Z. A. Mehrizi, M. Haghighatafshar, Spect-mpi iterative denoising during the reconstruction process using a two-phase learned convolutional neural network, *EJNMMP physics* 11 (1) (2024) 1–22.
- [107] J. Huang, L. Yang, F. Wang, Y. Wu, Y. Nan, W. Wu, C. Wang, K. Shi, A. I. Aviles-Rivero, C.-B. Schönlieb, et al., Enhancing global sensitivity and uncertainty quantification in medical image reconstruction with monte carlo arbitrary-masked mamba, *Medical Image Analysis* 99 (2025) 103334.
- [108] Z. Yang, H. Zhang, D. Zhao, B. Wei, Y. Xu, Restore-rwkv: Efficient and effective medical image restoration with rwkv, *arXiv preprint arXiv:2407.11087* (2024).
- [109] X. Ying, H. Guo, K. Ma, J. Wu, Z. Weng, Y. Zheng, X2ct-gan: reconstructing ct from biplanar x-rays with generative adversarial networks, in: *Proceedings of the IEEE/CVF conference on computer vision and pattern recognition*, 2019, pp. 10619–10628.
- [110] H. Xie, H. Shan, W. Cong, C. Liu, X. Zhang, S. Liu, R. Ning, G. Wang, Deep efficient end-to-end reconstruction (deer) network for few-view breast ct image reconstruction, *IEEE Access* 8 (2020) 196633–196646. doi:10.1109/ACCESS.2020.3033795.
- [111] D. Hu, J. Liu, T. Lv, Q. Zhao, Y. Zhang, G. Quan, J. Feng, Y. Chen, L. Luo, Hybrid-domain neural network processing for sparse-view ct reconstruction, *IEEE Transactions on Radiation and Plasma Medical Sciences* 5 (1) (2020) 88–98.
- [112] R. Singh, S. R. Digumarthy, V. V. Muse, A. R. Kambadakone, M. A. Blake, A. Tabari, Y. Hoi, N. Akino, E. Angel, R. Madan, et al., Image quality and lesion detection on deep learning reconstruction and iterative reconstruction of submillisievert chest and abdominal ct, *American Journal of Roentgenology* 214 (3) (2020) 566–573.
- [113] S. L. Brady, A. T. Trout, E. Somasundaram, C. G. Anton, Y. Li, J. R. Dillman, Improving image quality and reducing radiation dose for pediatric ct by using deep learning reconstruction, *Radiology* 298 (1) (2021) 180–188.
- [114] D. Hu, Y. Zhang, J. Liu, S. Luo, Y. Chen, Dior: Deep iterative optimization-based residual-learning for limited-angle ct reconstruction, *IEEE Transactions on Medical Imaging* 41 (7) (2022) 1778–1790.
- [115] C. Ma, Z. Li, J. Zhang, Y. Zhang, H. Shan, Freeseed: Frequency-band-aware and self-guided network for sparse-view ct reconstruction, in: *International Conference on Medical Image Computing and Computer-Assisted Intervention*, Springer, 2023, pp. 250–259.
- [116] Y. Lin, J. Yang, H. Wang, X. Ding, W. Zhao, X. Li, C<sup>2</sup>rv: Cross-regional and cross-view learning for sparse-view cbct reconstruction, in: *Proceedings of the IEEE/CVF Conference on Computer Vision and Pattern Recognition (CVPR)*, 2024, pp. 11205–11214.
- [117] N. Pezzotti, S. Yousefi, M. S. Elmahdy, J. H. F. Van Gemert, C. Schuelke, M. Doneva, T. Nielsen, S. Kastrulin, B. P. Lelieveldt, M. J. Van Osch, et al., An adaptive intelligence algorithm for undersampled knee mri reconstruction, *IEEE Access* 8 (2020) 204825–204838.
- [118] D. Qiu, S. Zhang, Y. Liu, J. Zhu, L. Zheng, Super-resolution reconstruction of knee magnetic resonance imaging based on deep learning, *Computer methods and programs in biomedicine* 187 (2020) 105059.

- [119] R. Shaul, I. David, O. Shitrit, T. R. Raviv, Subsampled brain mri reconstruction by generative adversarial neural networks, *Medical Image Analysis* 65 (2020) 101747.
- [120] Y. Wu, Y. Ma, D. P. Capaldi, J. Liu, W. Zhao, J. Du, L. Xing, Incorporating prior knowledge via volumetric deep residual network to optimize the reconstruction of sparsely sampled mri, *Magnetic resonance imaging* 66 (2020) 93–103.
- [121] C. Han, L. Rundo, K. Murao, T. Noguchi, Y. Shimahara, Z. Á. Milacski, S. Koshino, E. Sala, H. Nakayama, S. Satoh, Madgan: Unsupervised medical anomaly detection gan using multiple adjacent brain mri slice reconstruction, *BMC bioinformatics* 22 (2021) 1–20.
- [122] N. Koonjoo, B. Zhu, G. C. Bagnall, D. Bhutto, M. Rosen, Boosting the signal-to-noise of low-field mri with deep learning image reconstruction, *Scientific reports* 11 (1) (2021) 8248.
- [123] T. Küstner, N. Fuin, K. Hammernik, A. Bustin, H. Qi, R. Hajhosseiny, P. G. Masci, R. Neji, D. Rueckert, R. M. Botnar, et al., Cinenet: deep learning-based 3d cardiac cine mri reconstruction with multi-coil complex-valued 4d spatio-temporal convolutions, *Scientific reports* 10 (1) (2020) 13710.
- [124] E. Z. Chen, C. Zhang, X. Chen, Y. Liu, T. Chen, S. Sun, Computationally efficient 3d mri reconstruction with adaptive mlp, in: *International Conference on Medical Image Computing and Computer-Assisted Intervention*, Springer, 2023, pp. 195–205.
- [125] L. Kang, B. Tang, J. Huang, J. Li, 3d-mri super-resolution reconstruction using multi-modality based on multi-resolution cnn, *Computer Methods and Programs in Biomedicine* 248 (2024) 108110.
- [126] W. Whiteley, W. K. Luk, J. Gregor, Directpet: full-size neural network pet reconstruction from sinogram data, *Journal of Medical Imaging* 7 (3) (2020) 032503–032503.
- [127] A. Mehranian, S. D. Wollenweber, M. D. Walker, K. M. Bradley, P. A. Fielding, K.-H. Su, R. Johnsen, F. Kotasidis, F. P. Jansen, D. R. McGowan, Image enhancement of whole-body oncology [18f]-fdg pet scans using deep neural networks to reduce noise, *European journal of nuclear medicine and molecular imaging* 49 (2) (2022) 539–549.
- [128] D. Deidda, A. M. Denis-Bacelar, A. J. Fenwick, K. M. Ferreira, W. Heetun, B. F. Hutton, D. R. McGowan, A. P. Robinson, J. Scuffham, K. Thielemans, et al., Triple modality image reconstruction of pet data using spect, pet, ct information increases lesion uptake in images of patients treated with radioembolization with 90 y micro-spheres, *EJNMMI physics* 10 (1) (2023) 30.
- [129] F. Hashimoto, Y. Onishi, K. Ote, H. Tashima, T. Yamaya, Fully 3d implementation of the end-to-end deep image prior-based pet image reconstruction using block iterative algorithm, *Physics in Medicine & Biology* 68 (15) (2023) 155009.
- [130] K. Gong, K. Johnson, G. El Fakhri, Q. Li, T. Pan, Pet image denoising based on denoising diffusion probabilistic model, *European Journal of Nuclear Medicine and Molecular Imaging* 51 (2) (2024) 358–368.
- [131] S. Mostafapour, F. Gholamiankhah, S. Maroufpour, M. Momennezhad, M. Asadinezhad, S. R. Zakavi, H. Arabi, H. Zaidi, Deep learning-guided attenuation correction in the image domain for myocardial perfusion spect imaging, *Journal of computational design and engineering* 9 (2) (2022) 434–447.
- [132] H. Chung, D. Ryu, M. T. McCann, M. L. Klasky, J. C. Ye, Solving 3d inverse problems using pre-trained 2d diffusion models, in: *Proceedings of the IEEE/CVF Conference on Computer Vision and Pattern Recognition*, 2023, pp. 22542–22551.

- [133] T. Wu, Y.-J. Yuan, L.-X. Zhang, J. Yang, Y.-P. Cao, L.-Q. Yan, L. Gao, Recent advances in 3d gaussian splatting, *Computational Visual Media* 10 (4) (2024) 613–642.
- [134] Y. Li, X. Fu, S. Zhao, R. Jin, S. K. Zhou, Sparse-view ct reconstruction with 3d gaussian volumetric representation, *arXiv preprint arXiv:2312.15676* (2023).
- [135] Y. Lin, H. Wang, J. Chen, X. Li, Learning 3d gaussians for extremely sparse-view cone-beam ct reconstruction, in: *International Conference on Medical Image Computing and Computer-Assisted Intervention*, Springer, 2024, pp. 425–435.
- [136] E. Nikolakis, U. Gupta, J. Vengosh, J. Bui, R. Marinescu, Gaspct: Gaussian splatting for novel ct projection view synthesis, *arXiv preprint arXiv:2404.03126* (2024).
- [137] Z. Gao, B. Planche, M. Zheng, X. Chen, T. Chen, Z. Wu, DDGS-CT: Direction-disentangled gaussian splatting for realistic volume rendering, in: *The Thirty-eighth Annual Conference on Neural Information Processing Systems*, 2024.  
URL <https://openreview.net/forum?id=mY0ZnS2s9u>
- [138] Y. Cai, Y. Liang, J. Wang, A. Wang, Y. Zhang, X. Yang, Z. Zhou, A. Yuille, Radiative gaussian splatting for efficient x-ray novel view synthesis, in: *European Conference on Computer Vision*, Springer, 2025, pp. 283–299.
- [139] S. Wu, Y. Guo, Y. Ji, J. Tong, Y. Lu, M. Li, S. Huang, Y. Ding, H. Lu, GBIR: A novel gaussian iterative method for medical image reconstruction (2024).  
URL <https://openreview.net/forum?id=AkCWbxnt11>
- [140] O. Ronneberger, P. Fischer, T. Brox, U-net: Convolutional networks for biomedical image segmentation, in: *Medical image computing and computer-assisted intervention–MICCAI 2015: 18th international conference, Munich, Germany, October 5–9, 2015, proceedings, part III 18*, Springer, 2015, pp. 234–241.
- [141] A. Gu, T. Dao, Mamba: Linear-time sequence modeling with selective state spaces, *arXiv preprint arXiv:2312.00752* (2023).
- [142] B. Peng, E. Alcaide, Q. Anthony, A. Albalak, S. Arcadinho, S. Biderman, H. Cao, X. Cheng, M. Chung, M. Grella, et al., Rwkvr: Reinventing rnns for the transformer era, *arXiv preprint arXiv:2305.13048* (2023).
- [143] K. H. Hohne, M. Bomans, M. Riemer, R. Schubert, U. Tiede, W. Lierse, A volume-based anatomical atlas, *IEEE Computer Graphics and Applications* 12 (04) (1992) 73–77.
- [144] M. Chen, A. E. Kaufman, R. Yagel, *Volume graphics*, Springer Science & Business Media, 2012.
- [145] V. Kushwaha, G. Nandi, et al., Study of prevention of mode collapse in generative adversarial network (gan), in: *2020 IEEE 4th Conference on Information & Communication Technology (CICT)*, IEEE, 2020, pp. 1–6.
- [146] J. Sohl-Dickstein, E. Weiss, N. Maheswaranathan, S. Ganguli, Deep unsupervised learning using nonequilibrium thermodynamics, in: *International conference on machine learning*, pmlr, 2015, pp. 2256–2265.
- [147] J. Ho, A. Jain, P. Abbeel, Denoising diffusion probabilistic models, *Advances in neural information processing systems* 33 (2020) 6840–6851.
- [148] J. Song, C. Meng, S. Ermon, Denoising diffusion implicit models, *arXiv preprint arXiv:2010.02502* (2020).

- [149] R. Rombach, A. Blattmann, D. Lorenz, P. Esser, B. Ommer, High-resolution image synthesis with latent diffusion models, in: *Proceedings of the IEEE/CVF conference on computer vision and pattern recognition*, 2022, pp. 10684–10695.
- [150] K. E. Stull, M. L. Tise, Z. Ali, D. R. Fowler, Accuracy and reliability of measurements obtained from computed tomography 3d volume rendered images, *Forensic science international* 238 (2014) 133–140.
- [151] G. Zheng, Effective incorporating spatial information in a mutual information based 3d–2d registration of a ct volume to x-ray images, *Computerized medical imaging and graphics* 34 (7) (2010) 553–562.
- [152] F. Xu, K. Mueller, Real-time 3d computed tomographic reconstruction using commodity graphics hardware, *Physics in Medicine & Biology* 52 (12) (2007) 3405.
- [153] K. Engel, M. Hadwiger, J. M. Kniss, A. E. Lefohn, C. R. Salama, D. Weiskopf, Real-time volume graphics, in: *ACM Siggraph 2004 Course Notes*, 2004, pp. 29–es.
- [154] G. Chen, W. Wang, A survey on 3d gaussian splatting, *arXiv preprint arXiv:2401.03890* (2024).
- [155] C. Wang, K. Shang, H. Zhang, Q. Li, S. K. Zhou, Dudotrans: dual-domain transformer for sparse-view ct reconstruction, in: *International Workshop on Machine Learning for Medical Image Reconstruction*, Springer, 2022, pp. 84–94.
- [156] B. Song, L. Shen, L. Xing, Piner: Prior-informed implicit neural representation learning for test-time adaptation in sparse-view ct reconstruction, in: *2023 IEEE/CVF Winter Conference on Applications of Computer Vision (WACV)*, 2023, pp. 1928–1937. doi:10.1109/WACV56688.2023.00197.
- [157] K. Gong, C. Catana, J. Qi, Q. Li, Direct reconstruction of linear parametric images from dynamic pet using nonlocal deep image prior, *IEEE transactions on medical imaging* 41 (3) (2021) 680–689.
- [158] S. Makkar, S. Ye, M. Béguin, G. Dissertori, J. Hrbacek, A. Lomax, K. McNamara, C. Ritzler, D. C. Weber, L. Xing, et al., Partial-ring pet image correction using implicit neural representation learning.
- [159] L. Shen, J. Pauly, L. Xing, Nerp: implicit neural representation learning with prior embedding for sparsely sampled image reconstruction, *IEEE Transactions on Neural Networks and Learning Systems* 35 (1) (2022) 770–782.
- [160] Z. Liu, Y. Fang, C. Li, H. Wu, Y. Liu, D. Shen, Z. Cui, Geometry-aware attenuation learning for sparse-view cbct reconstruction, *IEEE Transactions on Medical Imaging* (2024).
- [161] Z. Guo, Z. Fang, Z. Fu, Ulre-nerf: 3d ultrasound imaging through neural rendering with ultrasound reflection direction parameterization, *arXiv preprint arXiv:2408.00860* (2024).
- [162] R. Dagli, A. Hibi, R. G. Krishnan, P. N. Tyrrell, Nerf-us: Removing ultrasound imaging artifacts from neural radiance fields in the wild, *arXiv preprint arXiv:2408.10258* (2024).
- [163] P.-H. Yeung, L. Hesse, M. Aliasi, M. Haak, W. Xie, A. I. Namburete, et al., Implicitvol: Sensorless 3d ultrasound reconstruction with deep implicit representation, *arXiv preprint arXiv:2109.12108* (2021).
- [164] R. Zha, Y. Zhang, H. Li, Naf: neural attenuation fields for sparse-view cbct reconstruction, in: *International Conference on Medical Image Computing and Computer-Assisted Intervention*, Springer, 2022, pp. 442–452.

- [165] M. Sun, Y. Zhu, H. Li, J. Ye, N. Li, Acnerf: enhancement of neural radiance field by alignment and correction of pose to reconstruct new views from a single x-ray, *Physics in Medicine & Biology* 69 (4) (2024) 045016.
- [166] J. Hu, Q. Fan, S. Hu, S. Lyu, X. Wu, X. Wang, Umednerf: Uncertainty-aware single view volumetric rendering for medical neural radiance fields, in: *2024 IEEE International Symposium on Biomedical Imaging (ISBI)*, IEEE, 2024, pp. 1–4.
- [167] J. Liu, X. Bai, VolumeNeRF: CT Volume Reconstruction from a Single Projection View , in: *proceedings of Medical Image Computing and Computer Assisted Intervention – MICCAI 2024*, Vol. LNCS 15007, Springer Nature Switzerland, 2024.
- [168] Y. Cai, J. Wang, A. Yuille, Z. Zhou, A. Wang, Structure-aware sparse-view x-ray 3d reconstruction, in: *Proceedings of the IEEE/CVF Conference on Computer Vision and Pattern Recognition*, 2024, pp. 11174–11183.
- [169] K. Iddrisu, S. Malec, A. Crimi, 3d reconstructions of brain from mri scans using neural radiance fields, in: *International Conference on Artificial Intelligence and Soft Computing*, Springer, 2023, pp. 207–218.
- [170] J. Feng, R. Feng, Q. Wu, X. Shen, L. Chen, X. Li, L. Feng, J. Chen, Z. Zhang, C. Liu, et al., Spatiotemporal implicit neural representation for unsupervised dynamic mri reconstruction, *IEEE Transactions on Medical Imaging* (2025).
- [171] J. Xu, D. Moyer, B. Gagoski, J. E. Iglesias, P. E. Grant, P. Golland, E. Adalsteinsson, Nesvor: implicit neural representation for slice-to-volume reconstruction in mri, *IEEE transactions on medical imaging* 42 (6) (2023) 1707–1719.
- [172] Z. Chen, L. Yang, J.-H. Lai, X. Xie, Cunerf: Cube-based neural radiance field for zero-shot medical image arbitrary-scale super resolution, in: *Proceedings of the IEEE/CVF International Conference on Computer Vision*, 2023, pp. 21185–21195.
- [173] C. Rao, Q. Wu, P. Zhou, J. Yu, Y. Zhang, X. Lou, An energy-efficient accelerator for medical image reconstruction from implicit neural representation, *IEEE Transactions on Circuits and Systems I: Regular Papers* 70 (4) (2022) 1625–1638.
- [174] J. Shi, J. Zhu, D. M. Pelt, K. J. Batenburg, M. B. Blaschko, Implicit neural representations for robust joint sparse-view ct reconstruction, *arXiv preprint arXiv:2405.02509* (2024).
- [175] B. Adlam, J. Lee, L. Xiao, J. Pennington, J. Snoek, Exploring the uncertainty properties of neural networks’ implicit priors in the infinite-width limit, *arXiv preprint arXiv:2010.07355* (2020).
- [176] Y. Lin, Z. Luo, W. Zhao, X. Li, Learning deep intensity field for extremely sparse-view cbct reconstruction, in: *International Conference on Medical Image Computing and Computer-Assisted Intervention*, Springer, 2023, pp. 13–23.
- [177] Z. Wang, A. C. Bovik, H. R. Sheikh, E. P. Simoncelli, Image quality assessment: from error visibility to structural similarity, *IEEE transactions on image processing* 13 (4) (2004) 600–612.
- [178] L. S. Chow, R. Paramesran, Review of medical image quality assessment, *Biomedical signal processing and control* 27 (2016) 145–154.
- [179] W. Wuest, M. May, M. Brand, N. Bayerl, A. Krauss, M. Uder, M. Lell, Improved image quality in head and neck ct using a 3d iterative approach to reduce metal artifact, *American Journal of Neuroradiology* 36 (10) (2015) 1988–1993.





- [197] L. M. Prevedello, S. S. Halabi, G. Shih, C. C. Wu, M. D. Kohli, F. H. Chokshi, B. J. Erickson, J. Kalpathy-Cramer, K. P. Andriole, A. E. Flanders, Challenges related to artificial intelligence research in medical imaging and the importance of image analysis competitions, *Radiology: Artificial Intelligence* 1 (1) (2019) e180031.
- [198] F. Zhuang, Z. Qi, K. Duan, D. Xi, Y. Zhu, H. Zhu, H. Xiong, Q. He, A comprehensive survey on transfer learning, *Proceedings of the IEEE* 109 (1) (2020) 43–76.
- [199] H. E. Kim, A. Cosa-Linan, N. Santhanam, M. Jannesari, M. E. Maros, T. Ganslandt, Transfer learning for medical image classification: a literature review, *BMC medical imaging* 22 (1) (2022) 69.
- [200] D. Karimi, S. K. Warfield, A. Gholipour, Transfer learning in medical image segmentation: New insights from analysis of the dynamics of model parameters and learned representations, *Artificial intelligence in medicine* 116 (2021) 102078.
- [201] M. Raghu, C. Zhang, J. Kleinberg, S. Bengio, Transfusion: Understanding transfer learning for medical imaging, *Advances in neural information processing systems* 32 (2019).
- [202] A. Kirillov, E. Mintun, N. Ravi, H. Mao, C. Rolland, L. Gustafson, T. Xiao, S. Whitehead, A. C. Berg, W.-Y. Lo, et al., Segment anything, in: *Proceedings of the IEEE/CVF international conference on computer vision*, 2023, pp. 4015–4026.
- [203] J. Ma, Y. He, F. Li, L. Han, C. You, B. Wang, Segment anything in medical images, *Nature Communications* 15 (1) (2024) 654.
- [204] Y. Zhang, M. An, Deep learning-and transfer learning-based super resolution reconstruction from single medical image, *Journal of healthcare engineering* 2017 (1) (2017) 5859727.
- [205] F. Knoll, K. Hammernik, E. Kobler, T. Pock, M. P. Recht, D. K. Sodickson, Assessment of the generalization of learned image reconstruction and the potential for transfer learning, *Magnetic resonance in medicine* 81 (1) (2019) 116–128.
- [206] J. Chen, X. Ran, Deep learning with edge computing: A review, *Proceedings of the IEEE* 107 (8) (2019) 1655–1674.
- [207] Y. Zheng, Y. Chen, B. Qian, X. Shi, Y. Shu, J. Chen, A review on edge large language models: Design, execution, and applications, *ACM Computing Surveys* 57 (8) (2025) 1–35.
- [208] A. Isosalo, J. Islam, H. Mustonen, E. Räninä, S. I. Inkinen, M. Brix, T. Kumar, J. Reponen, M. T. Nieminen, E. Harjula, Local edge computing for radiological image reconstruction and computer-assisted detection: A feasibility study, *Finnish Journal of eHealth and eWelfare* 15 (1) (2023) 52–66.
- [209] J. Zhang, D. Li, Q. Hua, X. Qi, Z. Wen, S. H. Myint, 3d remote healthcare for noisy ct images in the internet of things using edge computing, *IEEE Access* 9 (2021) 15170–15180.
- [210] S. Zhang, Y. Cui, D. Xu, Y. Lin, A collaborative inference strategy for medical image diagnosis in mobile edge computing environment, *PeerJ Computer Science* 11 (2025) e2708.
- [211] J. Gou, B. Yu, S. J. Maybank, D. Tao, Knowledge distillation: A survey, *International Journal of Computer Vision* 129 (6) (2021) 1789–1819.
- [212] F. Zhou, Y. Zhou, L. Wang, Y. Peng, D. E. Carlson, L. Tu, Distillation learning guided by image reconstruction for one-shot medical image segmentation, *arXiv preprint arXiv:2408.03616* (2024).
- [213] Z. Wu, X. Li, Adaptive knowledge distillation for high-quality unsupervised mri reconstruction with model-driven priors, *IEEE Journal of Biomedical and Health Informatics* 28 (6) (2024) 3571–3582.

- [214] S. M. Williamson, V. Prybutok, Balancing privacy and progress: a review of privacy challenges, systemic oversight, and patient perceptions in ai-driven healthcare, *Applied Sciences* 14 (2) (2024) 675.
- [215] D. Li, Z. Bian, S. Li, J. He, D. Zeng, J. Ma, Noise characteristics modeled unsupervised network for robust ct image reconstruction, *IEEE Transactions on Medical Imaging* 41 (12) (2022) 3849–3861.
- [216] H. K. Aggarwal, A. Pramanik, M. John, M. Jacob, Ensure: A general approach for unsupervised training of deep image reconstruction algorithms, *IEEE transactions on medical imaging* 42 (4) (2022) 1133–1144.
- [217] Y. Cai, J. Wang, A. Yuille, Z. Zhou, A. Wang, Structure-aware sparse-view x-ray 3d reconstruction (2024). [arXiv:2311.10959](https://arxiv.org/abs/2311.10959).  
URL <https://arxiv.org/abs/2311.10959>
- [218] H. U. Dike, Y. Zhou, K. K. Deveerasetty, Q. Wu, Unsupervised learning based on artificial neural network: A review, in: 2018 IEEE International Conference on Cyborg and Bionic Systems (CBS), IEEE, 2018, pp. 322–327.
- [219] H. Guan, P.-T. Yap, A. Bozoki, M. Liu, Federated learning for medical image analysis: A survey, *Pattern Recognition* (2024) 110424.
- [220] C.-M. Feng, Y. Yan, S. Wang, Y. Xu, L. Shao, H. Fu, Specificity-preserving federated learning for mr image reconstruction, *IEEE Transactions on Medical Imaging* 42 (7) (2022) 2010–2021.
- [221] G. Elmas, S. U. Dar, Y. Korkmaz, E. Ceyani, B. Susam, M. Ozbey, S. Avestimehr, T. Çukur, Federated learning of generative image priors for mri reconstruction, *IEEE Transactions on Medical Imaging* 42 (7) (2022) 1996–2009.
- [222] H. Guan, M. Liu, Domain adaptation for medical image analysis: a survey, *IEEE Transactions on Biomedical Engineering* 69 (3) (2021) 1173–1185.
- [223] Y. Han, J. Yoo, H. H. Kim, H. J. Shin, K. Sung, J. C. Ye, Deep learning with domain adaptation for accelerated projection-reconstruction mr, *Magnetic resonance in medicine* 80 (3) (2018) 1189–1205.
- [224] J. S. Yoon, K. Oh, Y. Shin, M. A. Mazurowski, H.-I. Suk, Domain generalization for medical image analysis: A review, *Proceedings of the IEEE* (2024).
- [225] Y. Zhao, T. Zhang, H. Ji, Test-time model adaptation for image reconstruction using self-supervised adaptive layers, in: *European Conference on Computer Vision*, Springer, 2024, pp. 111–128.
- [226] Y. He, A. Carass, L. Zuo, B. E. Dewey, J. L. Prince, Autoencoder based self-supervised test-time adaptation for medical image analysis, *Medical image analysis* 72 (2021) 102136.
- [227] A. Ziller, D. Usynin, R. Braren, M. Makowski, D. Rueckert, G. Kaissis, Medical imaging deep learning with differential privacy, *Scientific Reports* 11 (1) (2021) 13524.
- [228] Y. Yang, X. Xiao, X. Cai, W. Zhang, A secure and high visual-quality framework for medical images by contrast-enhancement reversible data hiding and homomorphic encryption, *IEEE Access* 7 (2019) 96900–96911.
- [229] F. Dutil, A. See, L. Di Jorio, F. Chandelier, Application of homomorphic encryption in medical imaging, *arXiv preprint arXiv:2110.07768* (2021).
- [230] P. Xi, X. Zhang, L. Wang, W. Liu, S. Peng, A review of blockchain-based secure sharing of healthcare data, *Applied Sciences* 12 (15) (2022) 7912.

- [231] M. Shen, Y. Deng, L. Zhu, X. Du, N. Guizani, Privacy-preserving image retrieval for medical iot systems: A blockchain-based approach, *Ieee Network* 33 (5) (2019) 27–33.
- [232] C. I. Eke, L. Shuib, The role of explainability and transparency in fostering trust in ai healthcare systems: a systematic literature review, open issues and potential solutions, *Neural Computing and Applications* (2024) 1–36.
- [233] Z. Salahuddin, H. C. Woodruff, A. Chatterjee, P. Lambin, Transparency of deep neural networks for medical image analysis: A review of interpretability methods, *Computers in biology and medicine* 140 (2022) 105111.
- [234] K. Li, Z. Wu, K.-C. Peng, J. Ernst, Y. Fu, Tell me where to look: Guided attention inference network, in: *Proceedings of the IEEE conference on computer vision and pattern recognition*, 2018, pp. 9215–9223.
- [235] O. Li, H. Liu, C. Chen, C. Rudin, Deep learning for case-based reasoning through prototypes: A neural network that explains its predictions, in: *Proceedings of the AAAI conference on artificial intelligence*, Vol. 32, 2018.
- [236] R. R. Selvaraju, M. Cogswell, A. Das, R. Vedantam, D. Parikh, D. Batra, Grad-cam: Visual explanations from deep networks via gradient-based localization, in: *Proceedings of the IEEE international conference on computer vision*, 2017, pp. 618–626.
- [237] M. Sundararajan, A. Taly, Q. Yan, Axiomatic attribution for deep networks, in: *International conference on machine learning*, PMLR, 2017, pp. 3319–3328.
- [238] H. Zhang, Q. Wang, J. Shi, S. Ying, Z. Wen, Deep unfolding network with spatial alignment for multi-modal mri reconstruction, *Medical Image Analysis* 99 (2025) 103331.